MSE 495 – Advanced Ceramics Technology

Michael Stuer (Empa) - Andrea Testino (PSI)

Week 5 – Perovskites

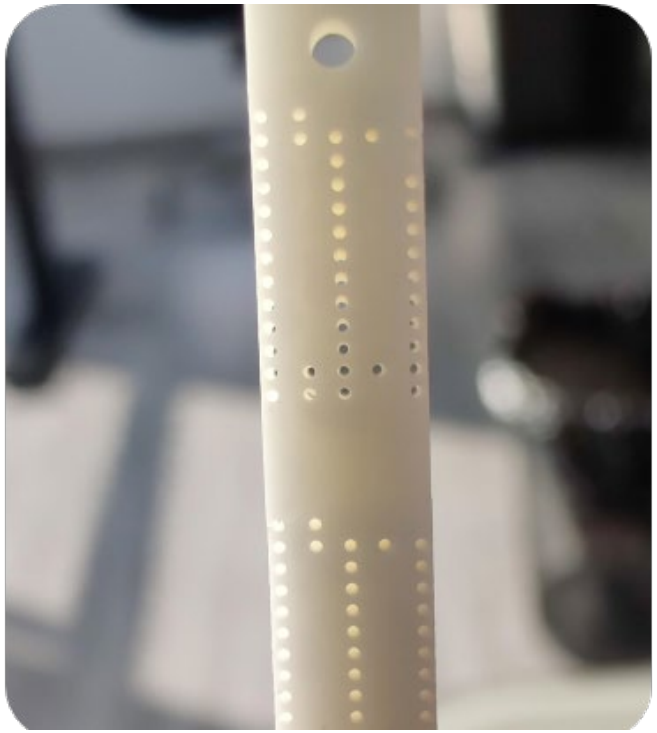

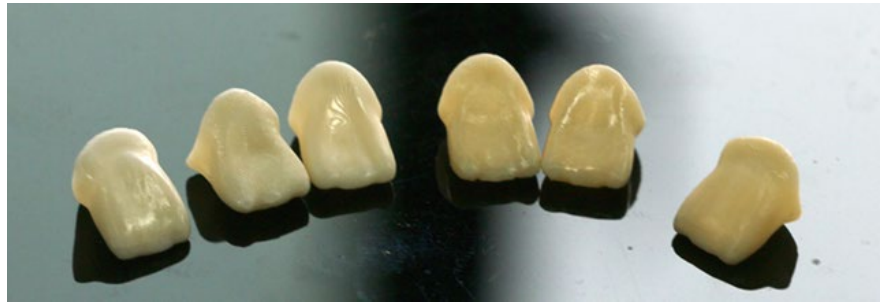

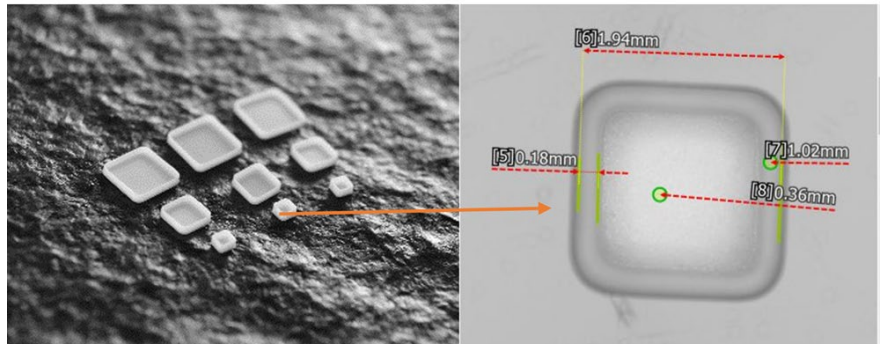

Perovskites*

Calcium titanate, $CaTiO_3$ or perovskite[1], is a natural mineral, prototype of a class of mineral with general formula ABX_3.

This class of materials has interesting properties, such as dielectric, piezoelectric, ferroelectric. In addition, there are examples of magnetic ordering, multiferroic properties, electronic conductivity (even superconductivity) and thermal and optical properties.

They are used in electrode material for SOFC due to high oxide ion conductivity and electron conductivity (and the combination thereof).

In addition, they show catalytic properties and redox behavior.

There are two major aspects that make these class of material interesting:

1. The crystal structure embrace a huge range variants from cubic (such as $SrTiO_3$), to hexagonal (such as $BaNiO_3$);
2. The properties can be tune over a wide range by substituting A, B or X. These allow a virtual infinite combination of compounds, including organic molecules, such as methylammonium lead iodine, a class of metal organic perovskites well-known in the recent years for their applications in photovoltaic cells.

Furthermore, thin films, superlattices, and nanoparticles shows unexpected response, when compared to bulk material of the same composition.

* R.J.D. Tilley "Perovskites. Structure-Property Relationship", Wiley, 2016 (ISBN: 9781118935668)

[1] Russian mineralogist Count Lev Aleksevich von Petrovski

Mercury: crystal structure visualization

Software download: https://www.ccdc.cam.ac.uk/solutions/software/free-mercury/

Brief introduction on View Symmetry Elements and Operation https://youtu.be/umx-CcRFDds

List of space groups: https://en.wikipedia.org/wiki/List_of_space_groups

Cubic, Pm-3m (221)


SrTiO3_19794.cif


BaTiO3_cubic_34900.cif

Hexagonal, P63/mmc (194)


BaNiO3_264690.cif

Tetragonal, P4mm (99)


BaTiO3_tetra_19801.cif


KCuF3 _tetra.cif

Orthorhombic, Pbnm (62)


CaTiO3_19790.cif

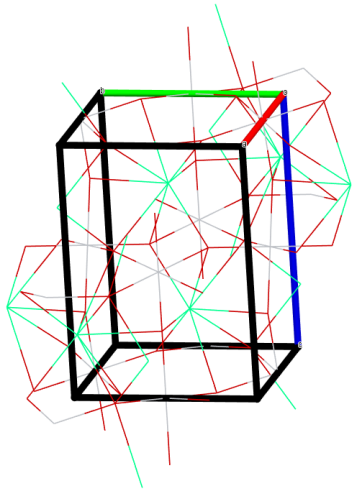

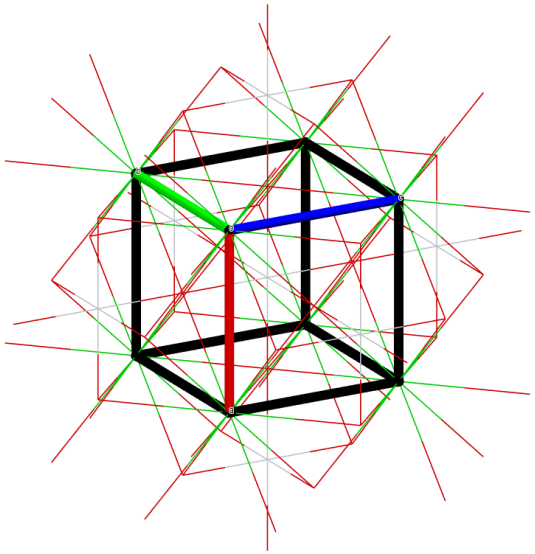

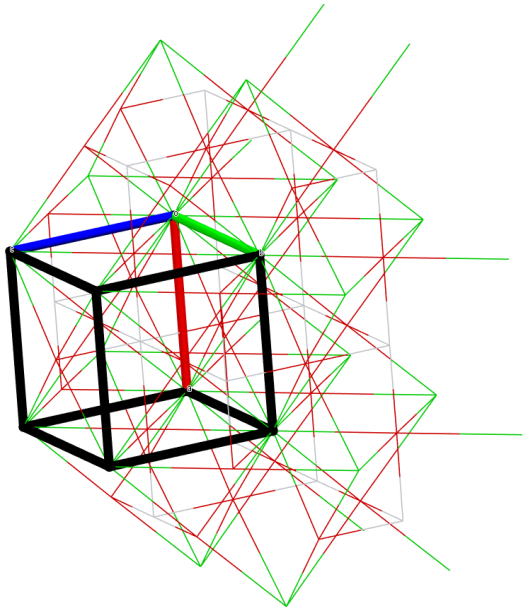

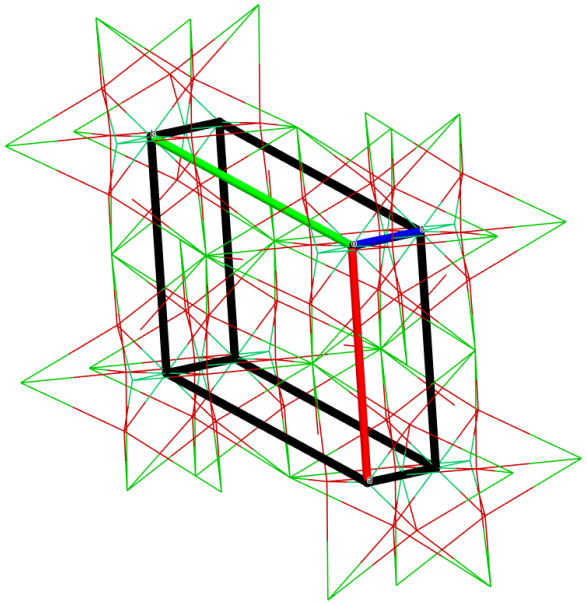

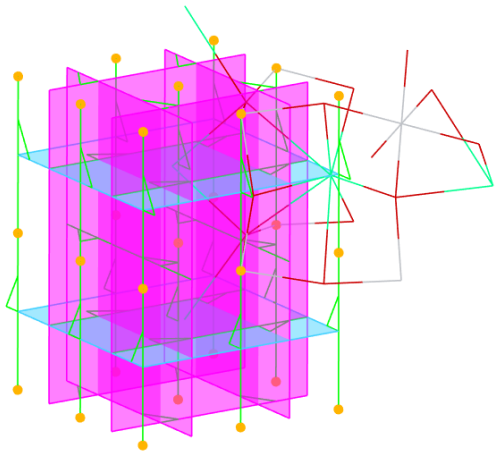

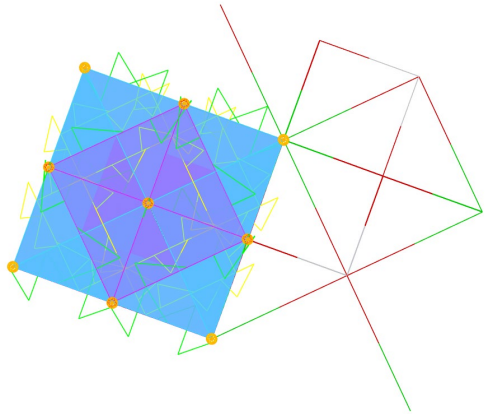

distortion

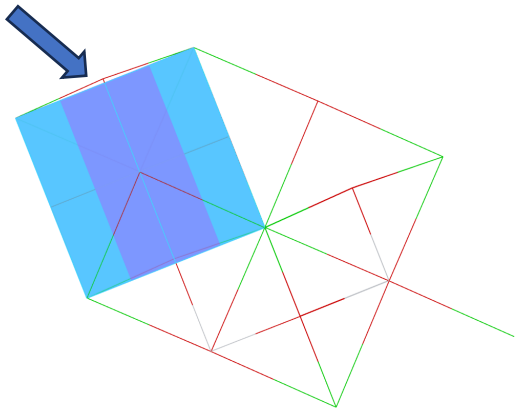

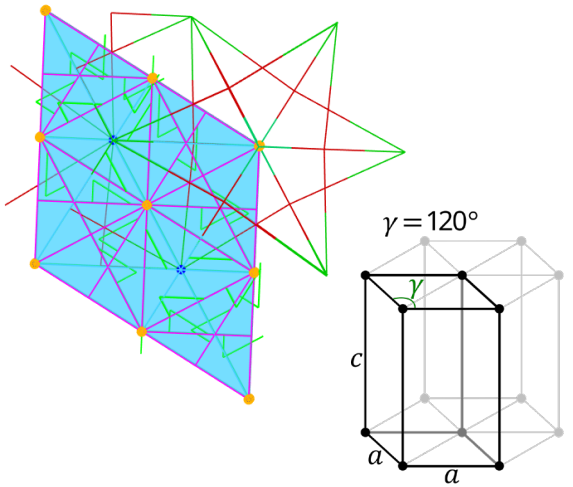

$CaTiO_3$, Orthorhombic

$SrTiO_3$, $BaTiO_3$, cubic

$BaTiO_3$, tetragonal

$BaNiO_3$, Hexagonal

Assuming simple ionic compounds, we might have

A, B = 1, 2 with X= -1

A, B = 1, 5 with X= -2
2, 4
3, 3

A, B = 4, 5 with X= -3

where usually

A is a large-size cation and (Ca, Ba, Sr, …)
B is a mediums-size cation (Ti, Zr, Ni, …)
X anion (O, halogen, …)

giving a neutral ionic structure.

Table 1.1 *Representative ABX_3 perovskite phases*[a]

Phase	Space group[b]	Unit cell		
		a (nm)	*b* (nm)	*c* (nm)
1, 2				
$AgMgF_3$	C, $Pm\bar{3}m$ (221)	0.41162		
$CsPbI_3$	C, $Pm\bar{3}m$ (221)	0.62894		
$KCuF_3$	T, *I*4/*mcm* (140)	0.56086		0.76281
$KMgF_3$	C, $Pm\bar{3}m$ (221)	0.39897		
$KZnF_3$	C, $Pm\bar{3}m$	0.40560		
$NaMgF_3$	O, *Pbnm* (62)	0.48904	0.52022	0.71403
$NaFeF_3$	O, *Pnma* (62)	0.56612	0.78801	0.54836
NH_4ZnF_3	C, $Pm\bar{3}m$ (221)	0.41162		
1, 5				
$KTaO_3$	C, $Pm\bar{3}m$ (221)	0.40316		
$KNbO_3$	O, *Amm*2 (38)	0.3971	0.5697	0.5723
2, 4				
$SrTiO_3$	C, $Pm\bar{3}m$ (221)	0.3905		
$BaTiO_3$	T, *P*4*mm* (99)	0.39906		0.40278
$CaTiO_3$	O, *Pbmn* (62)	0.54035	0.54878	0.76626
$BaSnO_3$	C, $Pm\bar{3}m$ (221)	0.4117		
$CdSnO_3$	O, *Pnma* (62)	0.52856	0.74501	0.51927
$CaIrO_3$	O, *Pbnm* (62)	0.52505	0.55929	0.76769
$PbTiO_3$	T, *P*4*mm* (99)	0.3902		0.4143
$PbZrO_3$	O, *Pbam* (55)	0.58822	1.17813	0.82293
$SrCoO_3$	C, $Pm\bar{3}m$ (221)	0.3855		
$SrMoO_3$	C, $Pm\bar{3}m$ (221)	0.39761		
$SrRuO_3$	O, *Pnma* (62)	0.55328	0.78471	0.55693
$(Fe,Mg)SiO_3$	O, *Pnma* (62)	0.5020	0.6900	0.4810
3, 3				
$BiFeO_3$	Tr, *R*3*c* (161)	0.55798		1.3867
$BiInO_3$	O, *Pnma* (62)	0.59546	0.83864	0.50619
$ErCoO_3$	O, *Pbnm* (62)	0.51212	0.54191	0.73519
$GdFeO_3$	O, *Pbnm* (62)	0.53490	0.56089	0.76687
$HoCrO_3$	O, *Pnma* (62)	0.5518	0.7539	0.5245
$LaAlO_3$	Tr, *R*3*c* (161)	0.53644		1.31195
$LaCoO_3$	Tr, $R\bar{3}c$ (167)	0.54437		1.30957
$LaMnO_3$	O, *Pbnm* (62)	0.55367	0.57473	0.76929
$LaTiO_3$	O, *Pbnm* (62)	0.5576	0.5542	0.7587
$NdAlO_3$	Tr, $R\bar{3}c$ (167)	0.53796		1.31386
$PrRuO_3$	O, *Pnma* (62)	0.58344	0.77477	0.53794
$YbMnO_3$	O, *Pbnm* (62)	0.52208	0.58033	0.73053
4, 5				
$ThTaN_3$	C, $Pm\bar{3}m$	0.4020		

[a] Many of these phases are polymorphic, and lattice parameters vary with temperature and pressure.
[b] The crystal system, here and throughout the other tables in this book, is abbreviated thus: C, cubic; H, hexagonal; M, monoclinic; O, orthorhombic; T, tetragonal; Tr, trigonal (often specified in terms of a hexagonal unit cell); Tri, triclinic.

$SrTiO_3$ – the aristotype* perovskite

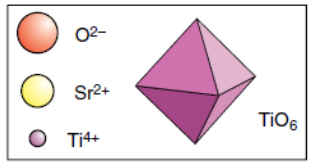

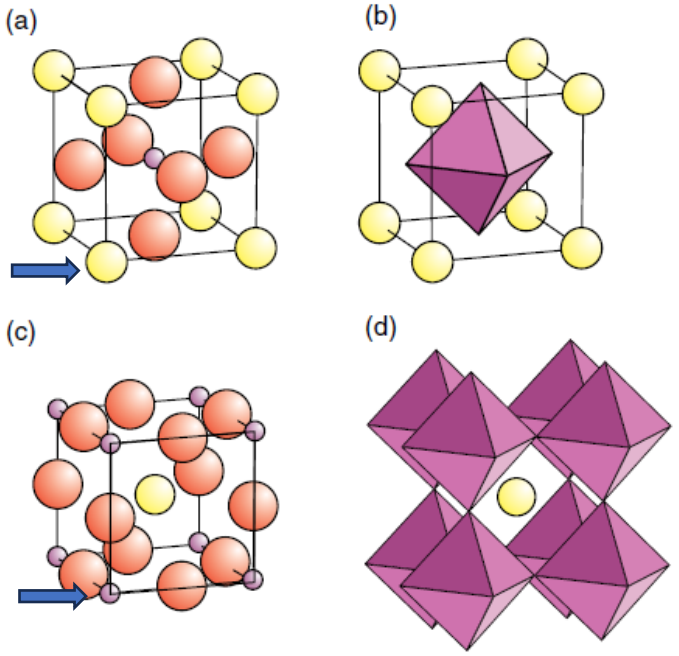

Origin on Sr^{2+}

Sr: 1 (*a*) 0,0,0;
Ti: 1 (*b*) ½,½,½;
O: 3 (*c*) ½,½,**0**; ½,**0**,½; **0**,½,½;

Origin on Ti^{4+}

Ti : 1 (*a*) 0,0,0;
Sr : 1 (*b*) ½,½,½;
O : 3 (*d*) ½,0,0; 0,½,0; 0,0,½;

Sr^{2+} is coordinated with 12 O^{2-}
Ti^{4+} is coordinated with 6 O^{2-}

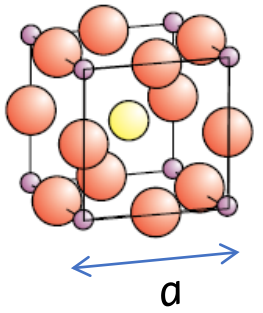

$$2(B - X) = a$$

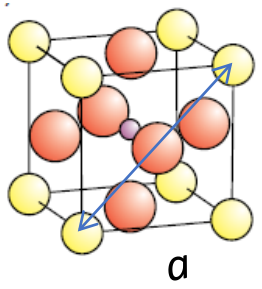

$$2(A - X) = \sqrt{2}a$$

$$\frac{(A - X)}{\sqrt{2}(B - X)} = 1$$

Goldschmidt, 1926

A-X : bond distance A – X
B-X : bond distance B – X

* Aristotype: High-symmetry crystal structure, ideal version of other structure with lower symmetry / higher complexity

Symmetry axes

3 tetrad axes

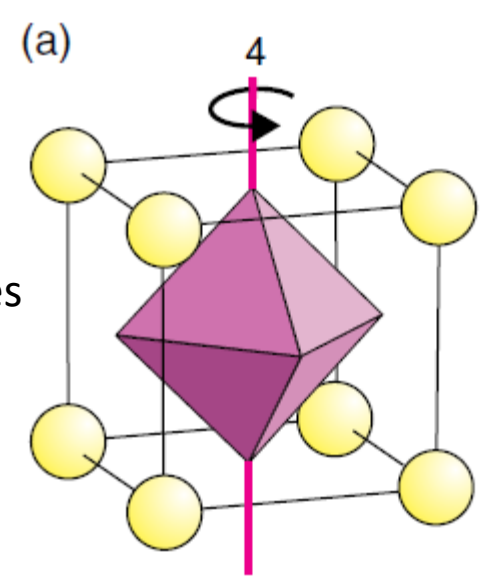

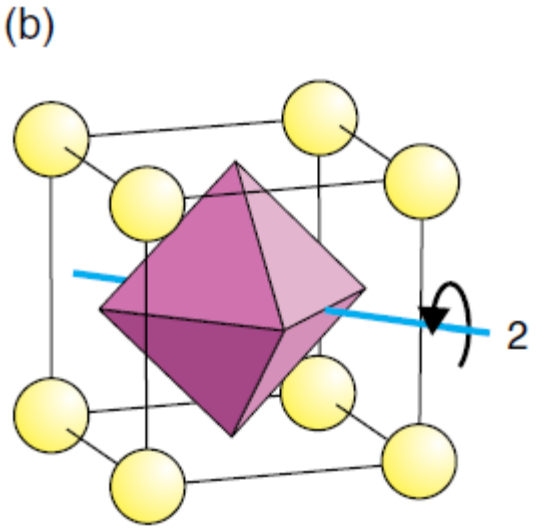

6 dial axes

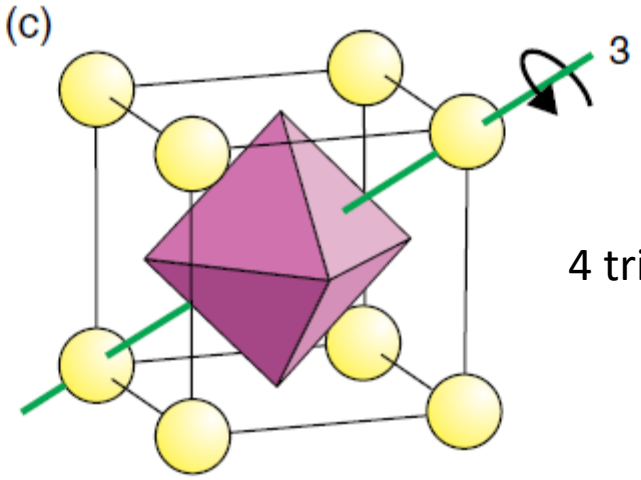

4 triad axes

The Goldschmidt tolerance factor (t)

In order evaluate the tolerance factor, the ionic radii are needed.

$$\frac{(A-X)}{\sqrt{2}(B-X)} = 1$$

$$t = \frac{(r_A + r_X)}{\sqrt{2}(r_B + r_X)}$$

Where r_A is the radius of the cage site cation, r_B is the radius of the octahedrally coordinated cation, and r_X is the radius of the anion.

Goldschmidt proposed that a perovskite structure would form if t ≈ 1

To make this estimation, it is necessary to use the radii of the appropriate coordination*, which has to be 12 for A, 6 for B, and linear (2) for X.
Since many perovskites are described, it is in use to consider the bond lengths in the crystal structure rather than the ionic radii and consider the observed tolerance factor:

$$t_{obs} = \frac{(A-X)}{\sqrt{2}(B-X)}$$

It is a simple but powerful method. If t in the range 0.9 - 1 a cubic perovskite structure is plausible. For t > 1, hexagonal packing is preferred. For 0.7 < t < 0.9, lower symmetry can be predicted. This works reasonably well for oxides. For chlorides and sulphides, the t values are lower with cubic structure for t = 0.8-0.9.

*https://en.wikipedia.org/wiki/Coordination_geometry

The Goldschmidt tolerance factor (t)

For complex perovskites, e.g., with different cations in A-site and different cation in B-site, the average bond lengths can be considered.

$$t_{obs} = \frac{\langle A - X \rangle}{\sqrt{2}\langle B - X \rangle}$$

In addition to the coordination*, the ionic radii dependent on the spin state** for the metals from Cr to Ni.

For instance: Fe^{3+}

Fe electronic configuration: $4s^2\ 3d^6$

Fe^{3+} electronic configuration : $4s^0\ 3d^5$

Fe^{3+},coord. 6, low spin = 55 pm
Fe^{3+},coord. 6, high spin = 64.5 pm

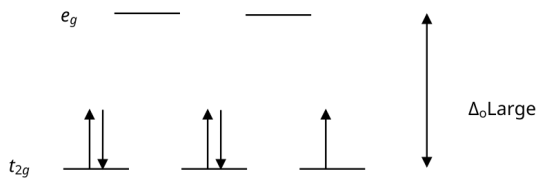

Low spin

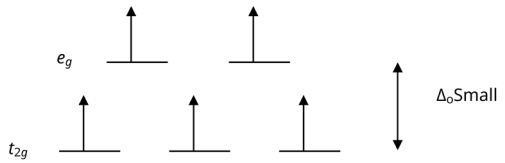

High spin

* https://en.wikipedia.org/wiki/Ionic_radius
** https://en.wikipedia.org/wiki/Spin_states_(d_electrons)

Electroceramics: concepts recall

Dielectric: insulator that can be polarized by an applied electric field (linear)

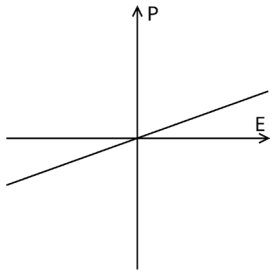

Dielectric

Paraelectric: non-linear P vs. E (centrosymmetric structures)

Ferroelectric: in analogy with ferromagnetic material, is a material that have a spontaneous electric polarization that can be reversed by the application of an external electric field. They show hysteresis.

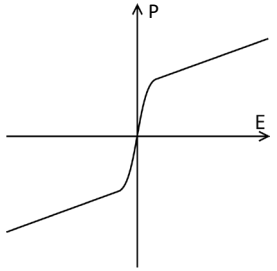

Paraelectric

<u>Piezoelectric</u> materials: applying a displacement we got a potential; applying a potential we got a displacement. E.g., lead zirconate titanate, (PZT, $Pb(Ti,Zr)O_3$) or lead-free ceramics, potassium sodium niobate, (KNN,$(K, Na)NbO_3$-based) materials.

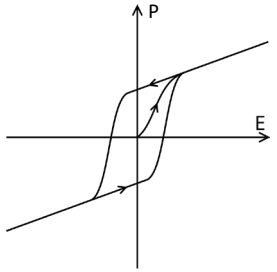

Ferroelectric

<u>Pyroelectric</u> materials (thermoelectric): applying a potential, we got a heat (cool) flow; applying a heat flow, we got a potential, e.g., lithium tantalate ($LiTaO_3$).

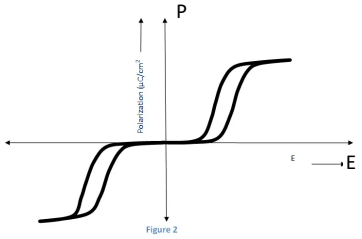

Antiferroelec.

If a material shows ferroelectric and ferromagnetic properties is called <u>multiferroic</u>.

Magnetic_orders.webm.480p.vp9.webm

Typically, material demonstrate ferroelectricity only below a certain temperature, called Curie temperature, Tc. They become paraelectric above Tc.

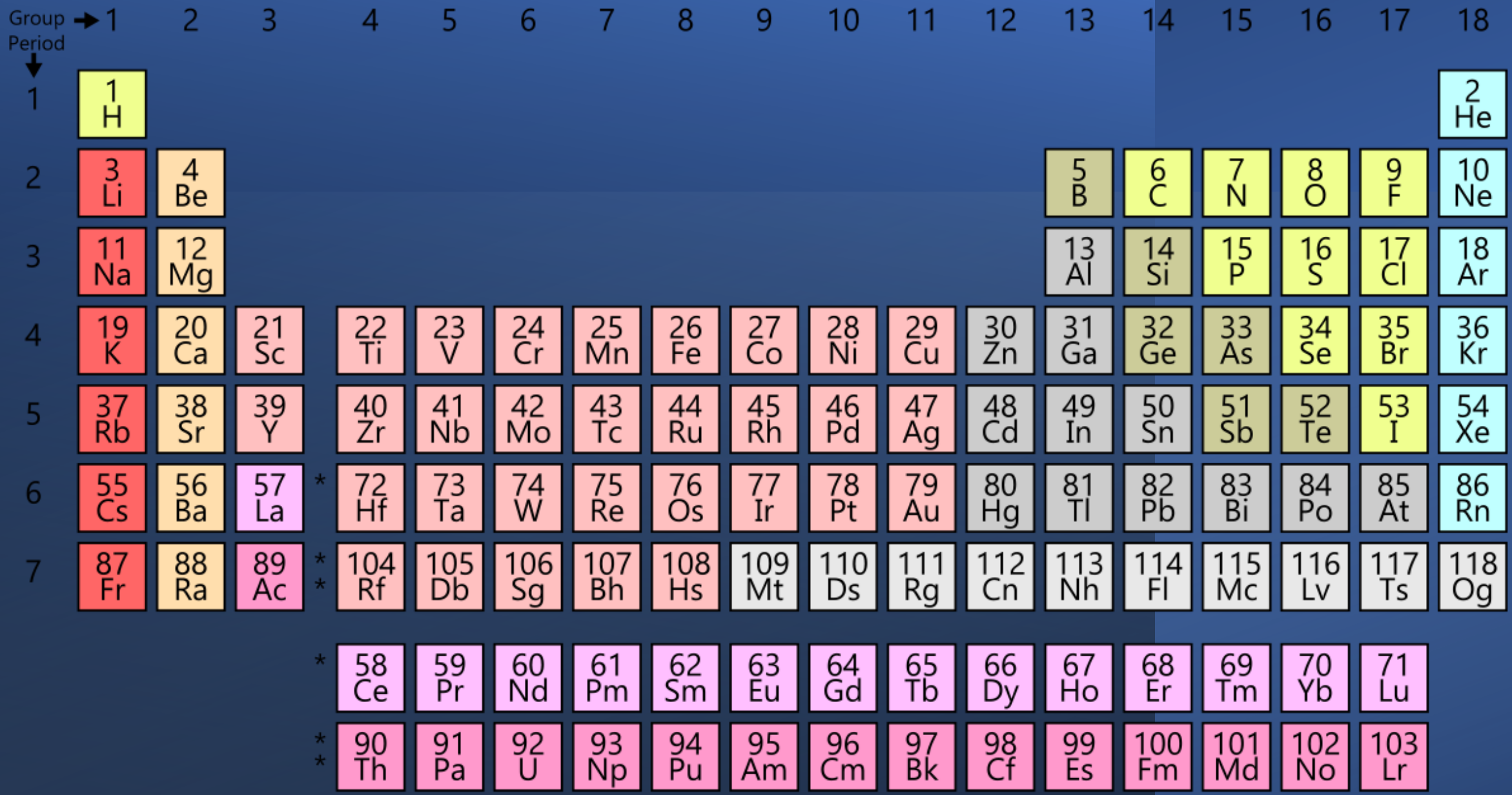
Group → 1 2 3 4 5 6 7 8 9 10 11 12 13 14 15 16 17 18
Period ↓
1 1 H 2 He
2 3 Li 4 Be 5 B 6 C 7 N 8 O 9 F 10 Ne
3 11 Na 12 Mg 13 Al 14 Si 15 P 16 S 17 Cl 18 Ar
4 19 K 20 Ca 21 Sc 22 Ti 23 V 24 Cr 25 Mn 26 Fe 27 Co 28 Ni 29 Cu 30 Zn 31 Ga 32 Ge 33 As 34 Se 35 Br 36 Kr
5 37 Rb 38 Sr 39 Y 40 Zr 41 Nb 42 Mo 43 Tc 44 Ru 45 Rh 46 Pd 47 Ag 48 Cd 49 In 50 Sn 51 Sb 52 Te 53 I 54 Xe
6 55 Cs 56 Ba 57 La * 72 Hf 73 Ta 74 W 75 Re 76 Os 77 Ir 78 Pt 79 Au 80 Hg 81 Tl 82 Pb 83 Bi 84 Po 85 At 86 Rn
7 87 Fr 88 Ra 89 Ac * 104 Rf 105 Db 106 Sg 107 Bh 108 Hs 109 Mt 110 Ds 111 Rg 112 Cn 113 Nh 114 Fl 115 Mc 116 Lv 117 Ts 118 Og
* 58 Ce 59 Pr 60 Nd 61 Pm 62 Sm 63 Eu 64 Gd 65 Tb 66 Dy 67 Ho 68 Er 69 Tm 70 Yb 71 Lu
* 90 Th 91 Pa 92 U 93 Np 94 Pu 95 Am 96 Cm 97 Bk 98 Cf 99 Es 100 Fm 101 Md 102 No 103 Lr

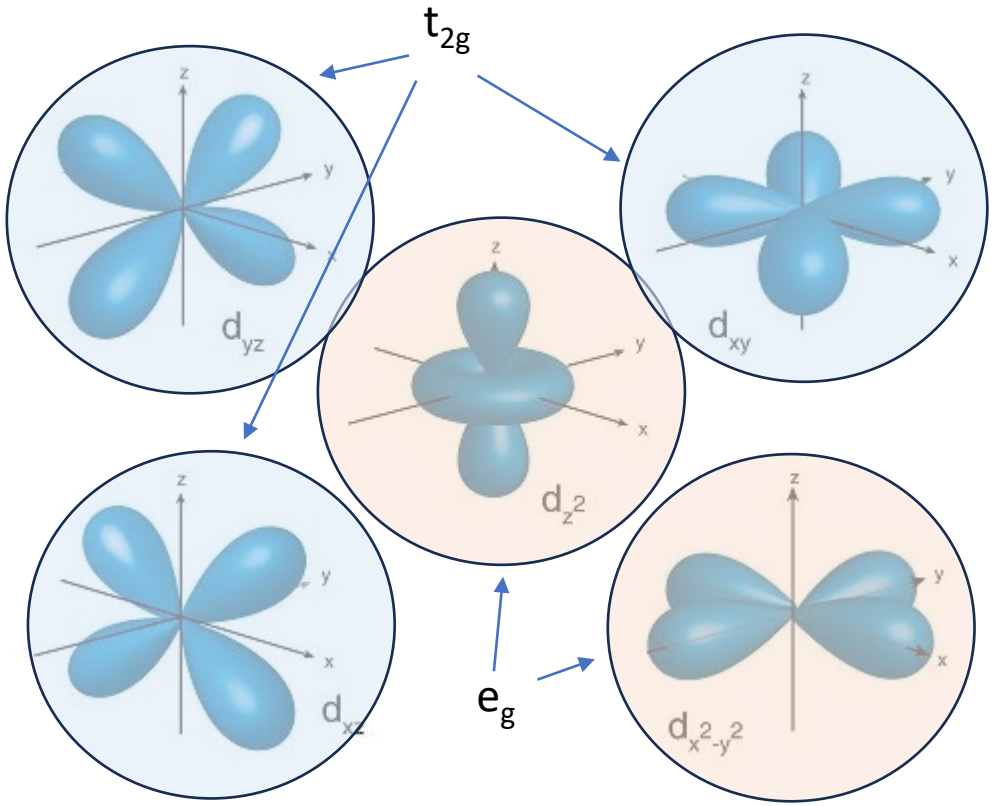

1. d orbitals “shape”

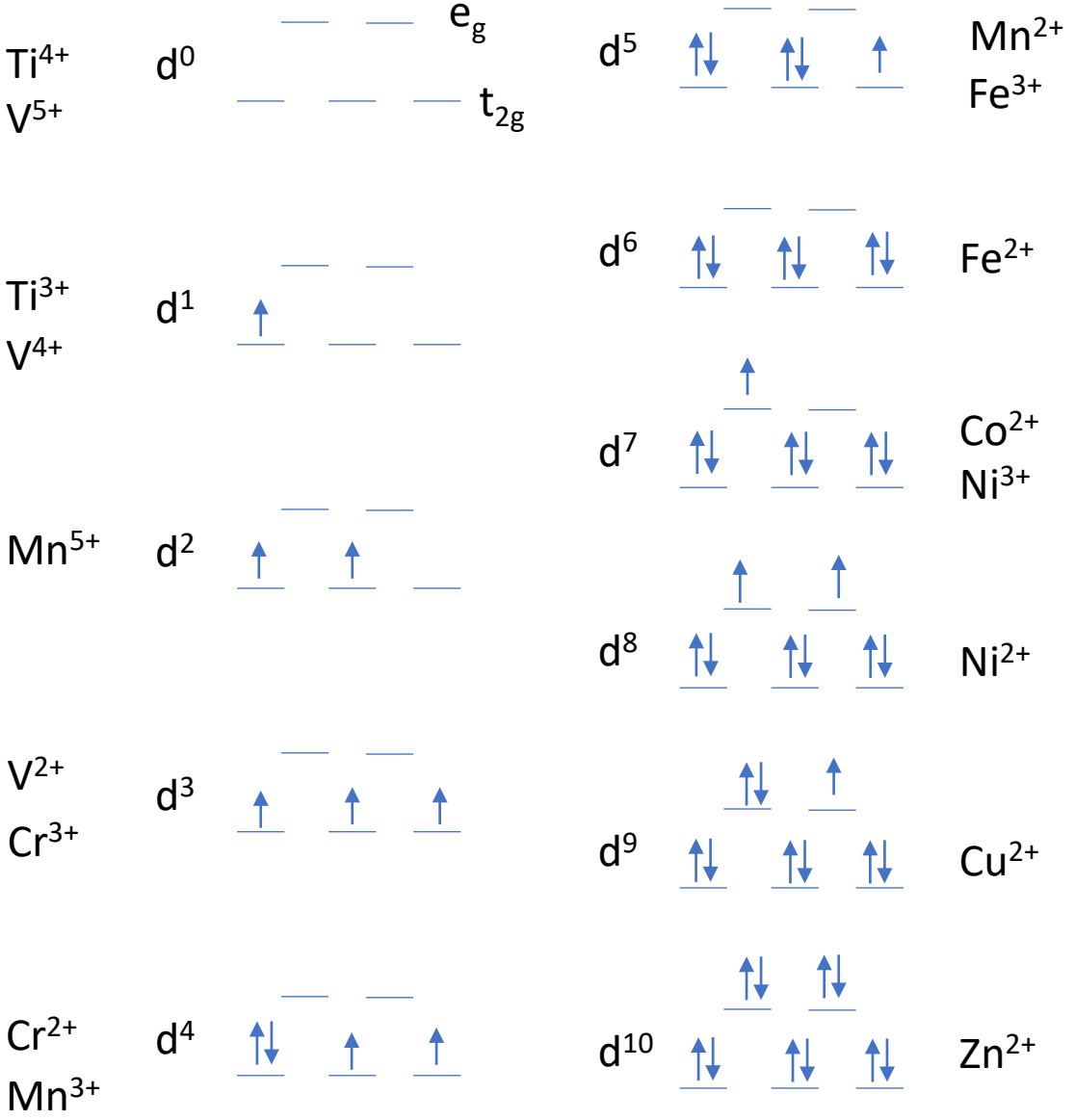

2. Hund’s and Pauli’s rules

d^4 

Low spin
t_{2g} degeneration

d^4 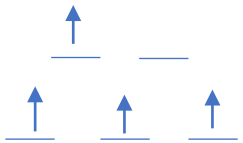

High spin
e_g degeneration

d^5 

ls
t_{2g} deg.

d^5 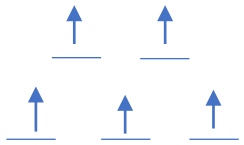

hs

d^6 

ls

d^6 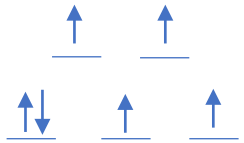

hs
t_{2g} deg.

d^7 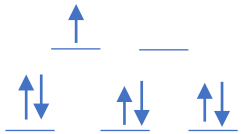

ls
e_g deg.

d^7 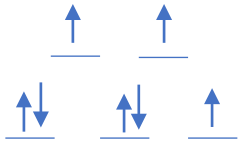

hs
t_{2g} deg.

d^9 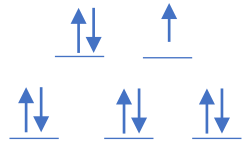

e_g deg.

Jahn-Teller distortion (first order) – applied to octahedrally coordinated transition metal **B-site** cations

Jahn–Teller theorem*: “Any molecule with a symmetrical atomic configuration and a degenerate electronic ground state is unstable and will distort so as to remove the electronic degeneracy.”
In the spherical filed, the 5 d orbitals have the same energy level. In an octahedral field, the degeneration is reduced, giving 2 energy levels: e_g (2 levels) and t_{2g} (3 levels). When electrons occupy these levels, we might have degeneracy in the e_g (with significant distortion) and t_{2g} (not significant distortion).

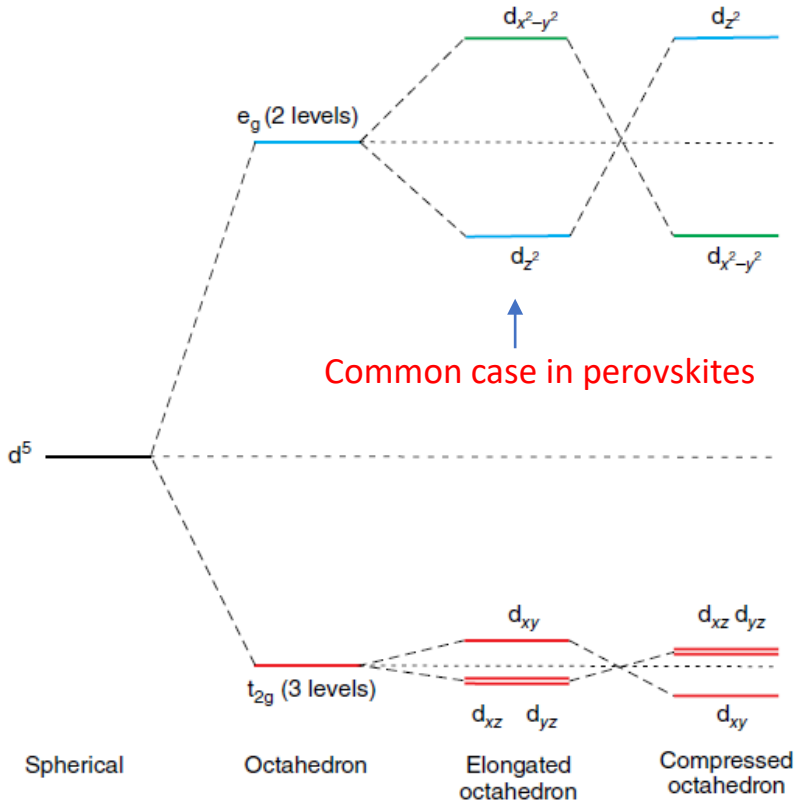

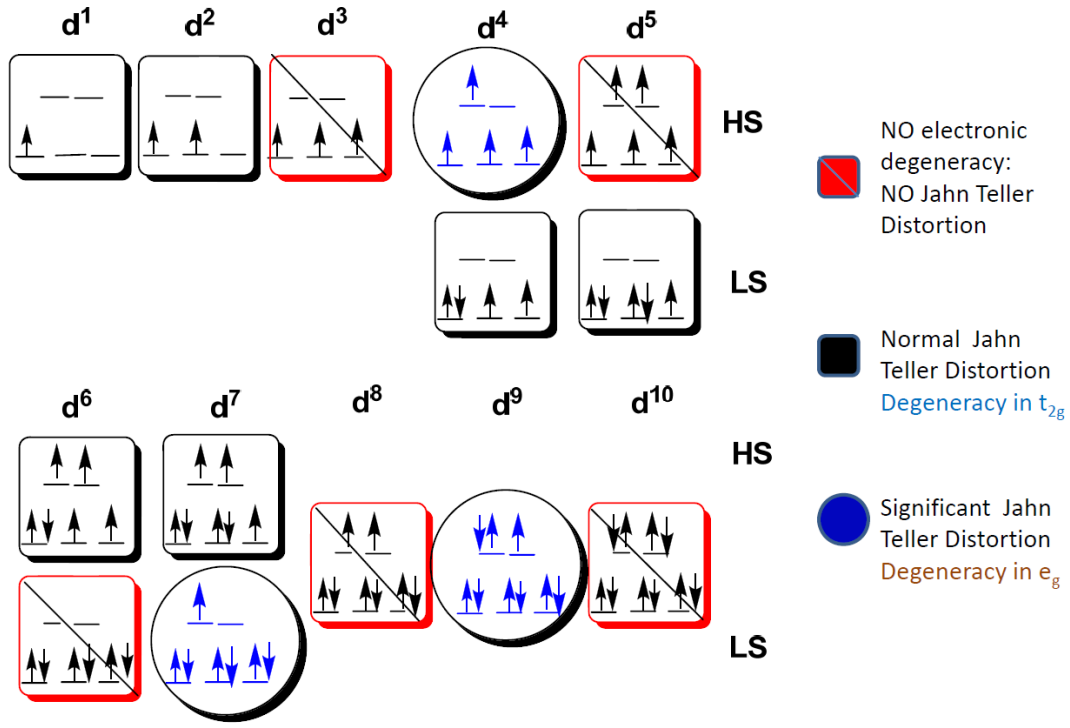

*H. Jahn and E. Teller (1937). "Stability of Polyatomic Molecules in Degenerate Electronic States. I. Orbital Degeneracy". Proceedings of the Royal Society A 161 (905): 220–235

Jahn-Teller distortion (first order) – applied to octahedrally coordinated transition metal **B-site** cations

A cation with odd number of electron in the e_g level, for instance Cr^{2+} (hs), Co^{2+} (ls), or Cu^{2+} will undergo distortion, compression or elongation, along one of the equivalent tilt axis. The energy difference in t_{2g} is rather small, may induce a negligible distortion. Instead, in the e_g case is significant and does lead to distortion. In perovskite, the distortion is generally elongation. This distortion does not influence, in general, the A and B positions but the cell symmetry drops to tetragonal or orthorhombic.

The J-T distortion is temperature and pressure sensitive, so high pressure and/or high temperature contrast the distortion, promoting the high symmetry configuration (cubic).

An example is given by $KCuF_3$. The J-T ion Cu^{2+} show degeneration of the e_g level. It is tetragonal at 295K and ambient pressure. At high pressure the distortion decreases.

$KCuF_3$ tetra

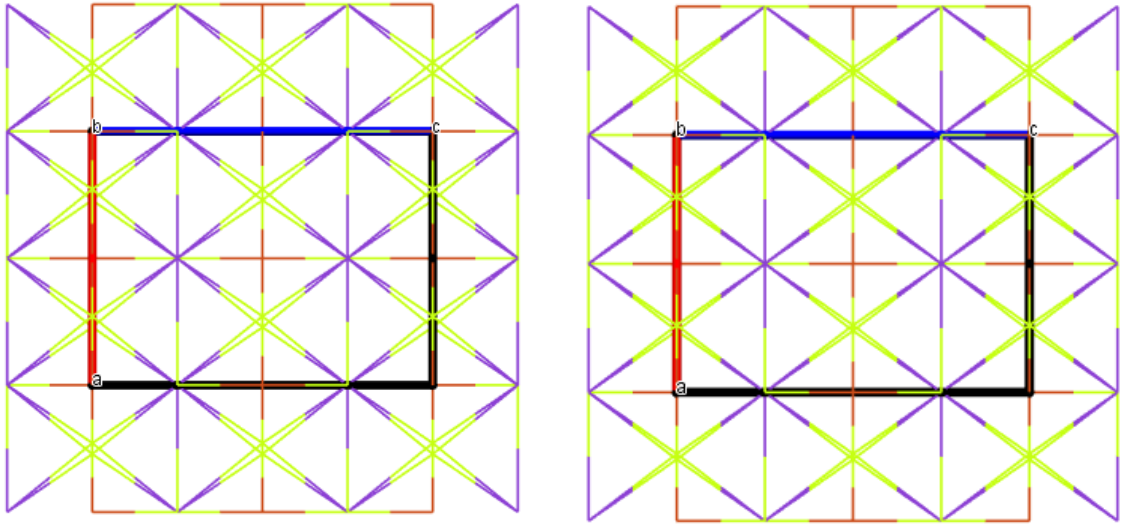

low pressure high pressure

$BaTiO_3$: Cation displacement - second order Jahn-Teller distortion (or pseudo J-T distortion)

In the 1940s the dielectric and ferroelectric properties of BT were discovered. What is the reason for the spontaneous electric polarization in BT?

Ti^{4+} : d^0 so it is not J-T ion. A symmetry change is provided by cation displacement along one of the symmetry axis of the octahedron (see slide 6).

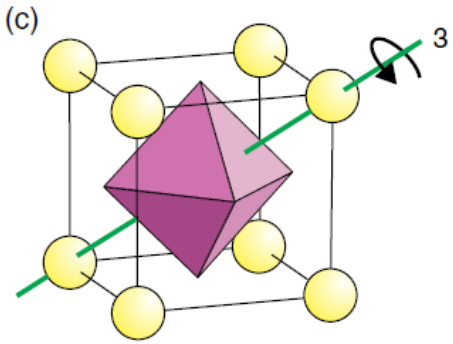

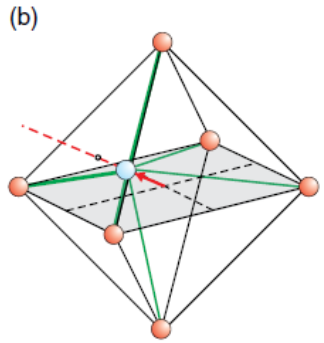

3 longer;
3 shorter.

triad axis

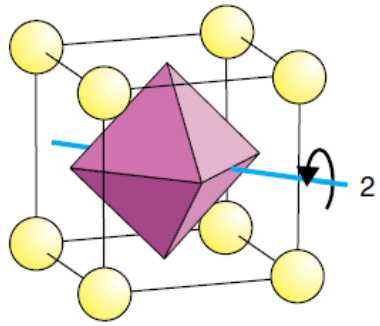

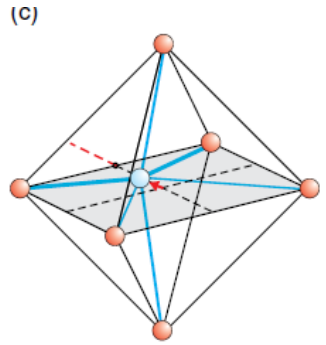

dial axes

2 longer;
2 shorter;
2 interm.

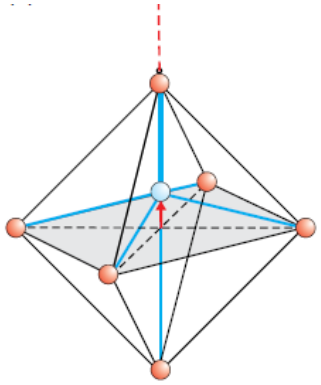

1 longer;
1 shorter;
4 interm.

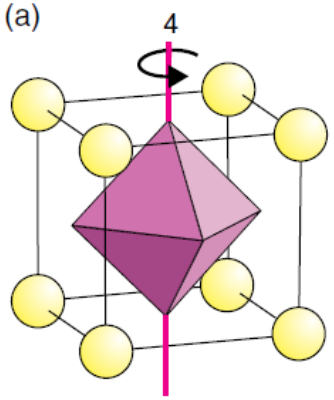

tetrad axis

$BaTiO_3$: phase transformation

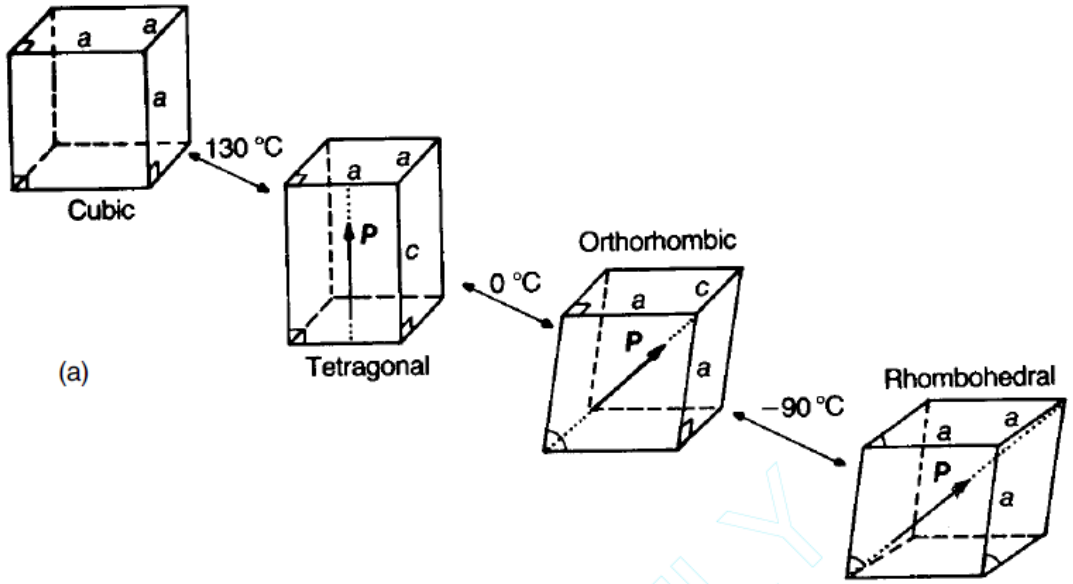

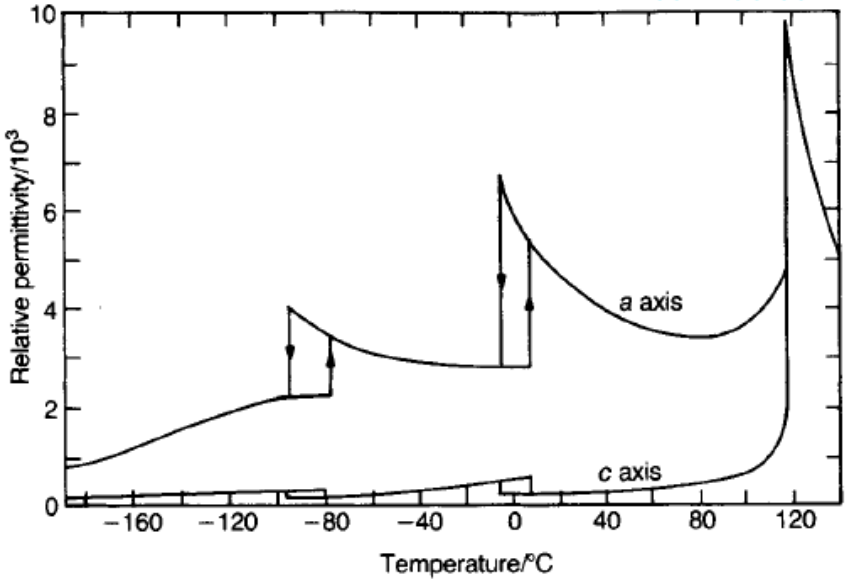

Above Tc, BT shows a cubic structure. The tolerance factor is slight larger than 1 and distortions take place.

Orthorhombic

Table 2 Ionic radii and tolerance factors of the synthesised perovskite-type catalysts

Perovskite ABO_3	Ionic radius [Å][a,b] Cation A		Cation B		Tolerance factor[c]
$CaTiO_3$	Ca^{2+} (VIII)	1.12	Ti^{4+} (VI)	0.605	0.89
$SrTiO_3$	Sr^{2+} (XII)	1.44	Ti^{4+} (VI)	0.605	1.00
$BaTiO_3$	Ba^{2+} (XII)	1.61	Ti^{4+} (VI)	0.605	1.06
$CaZrO_3$	Ca^{2+} (VIII)	1.12	Zr^{4+} (VI)	0.72	0.84
$SrZrO_3$	Sr^{2+} (XII)	1.44	Zr^{4+} (VI)	0.72	0.95
$BaZrO_3$	Ba^{2+} (XII)	1.61	Zr^{4+} (VI)	0.72	1.00
$CaCeO_3$	Ca^{2+} (VIII)	1.12	Ce^{4+} (VI)	0.87	0.78
$SrCeO_3$	Sr^{2+} (XII)	1.44	Ce^{4+} (VI)	0.87	0.88
$BaCeO_3$	Ba^{2+} (XII)	1.61	Ce^{4+} (VI)	0.87	0.94

Cubic or tetragonal

[a] Data from ref. 27. [b] Numbers in parentheses describe the coordination of the ion within the perovskite. [c] Ionic radius of O^{2-} (VI): 1.40 Å.

R.D. Shannon, *Acta Cryst.* (1976). A32, 751

$BaTiO_3$: distortion

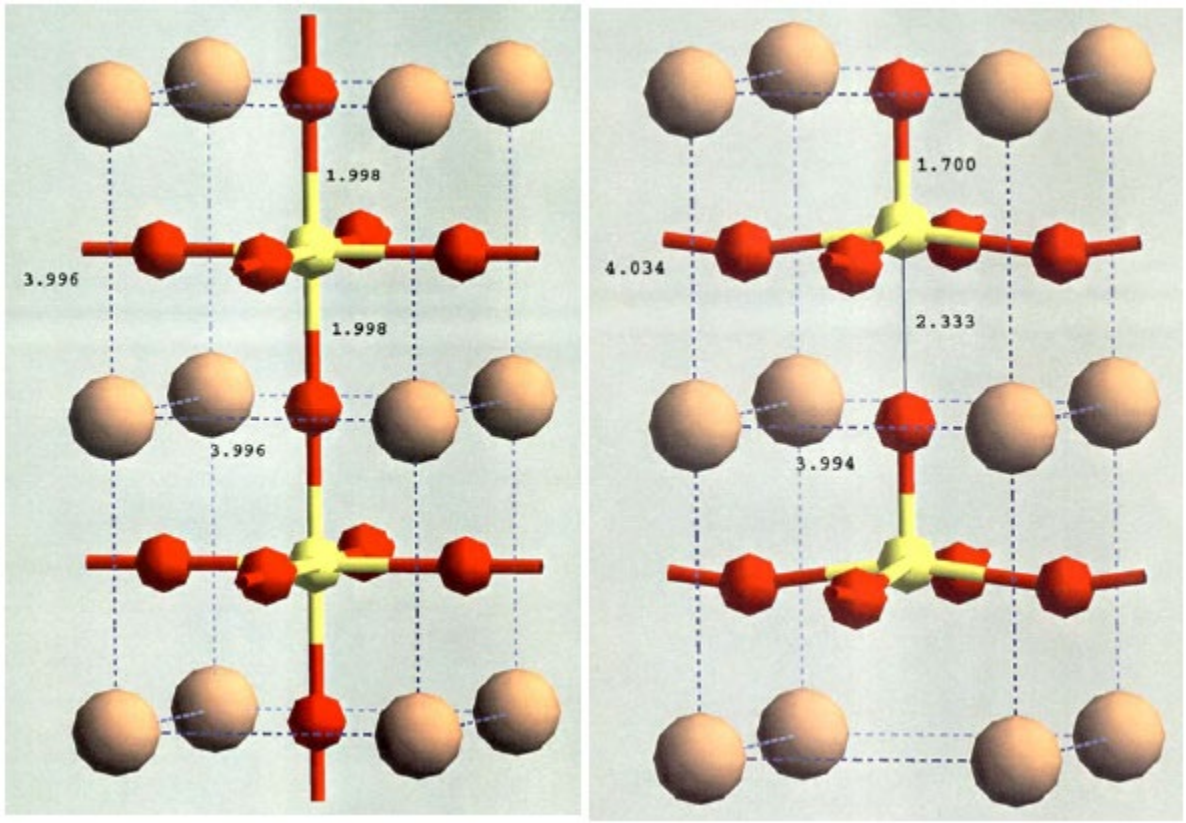

cubic tetragonal

As for first order J-T distortion, also these are P sensitive in the GPa range.

As the crystal cools through the cubic – tetragonal transition temperature, the cubic cell expands slightly along one edge to produce the tetragonal *c*-axis and is slightly compressed along the other two edges to form the tetragonal *a*- and *b*-axes. The change in the Ba^{2+} positions is almost negligible. The Ti^{4+} displacement is accompanied by a slight change in octahedron dimensions so that two equatorial oxygen atoms move parallel to the +c-axis and two move in the opposite direction. These displacements give rise to electric dipoles, **p**, one in each octahedron that are the source of the ferroelectric properties of tetragonal $BaTiO_3$. There is no preference as to which of the original cubic axes becomes the polar direction, and so this can take one of six equivalent directions, so that a single crystal invariably becomes heavily twinned on cooling. Other distortion take place at lower temperature but without practical relevance.

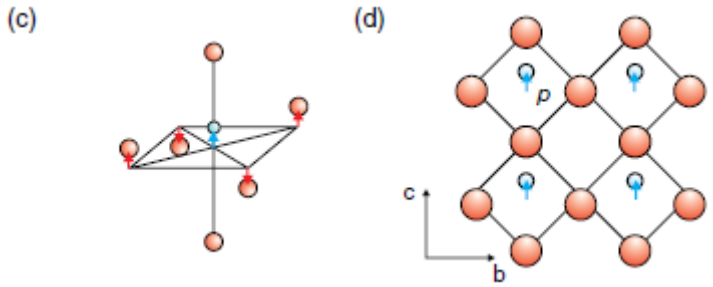

$BaTiO_3$: ferroelectric tetragonal structure.

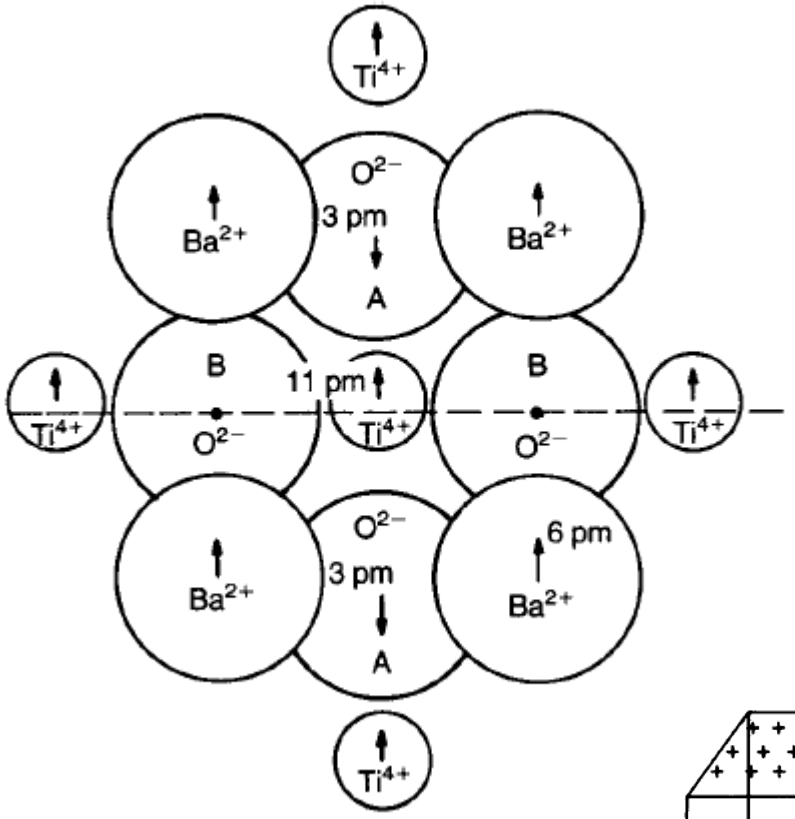

It is evident that if the central Ti^{4+} ion is closer to one of the O^{2-} ions marked A, it will be energetically favorable for the Ti^{4+} ion on the opposite side of A to be located more distantly from that O^{2-} ion, thus engendering a similar displacement of all the Ti^{4+} ions in a particular column in the same direction. Coupling between neighboring columns occurs in $BaTiO_3$ so that all the Ti^{4+} ions are displaced in the same direction.

An immediate consequence of the onset of spontaneous polarization in a body is the appearance of an apparent surface charge density and an accompanying depolarizing field ED (a).

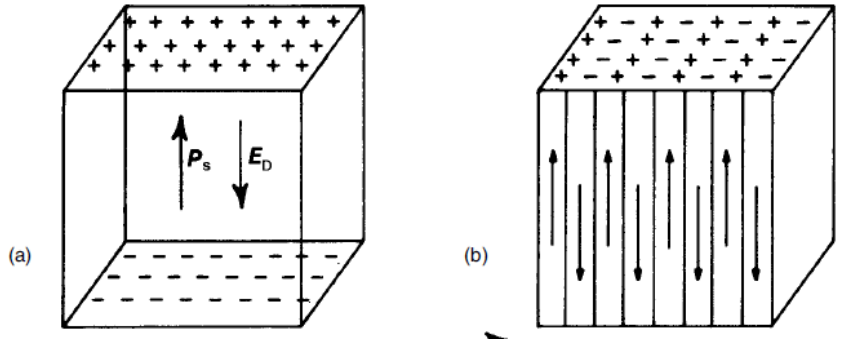

The energy associated with the polarization in the depolarizing field is minimized by twinning, a process in which the crystal is divided into many oppositely polarized regions, as shown in (b). These regions are called domains and the whole configuration shown comprises 180° domains. Thus, the surface consists of a mosaic of areas carrying apparent charges of opposite sign, resulting in a reduction in ED and in energy.

$BaTiO_3$: ferroelectric domains

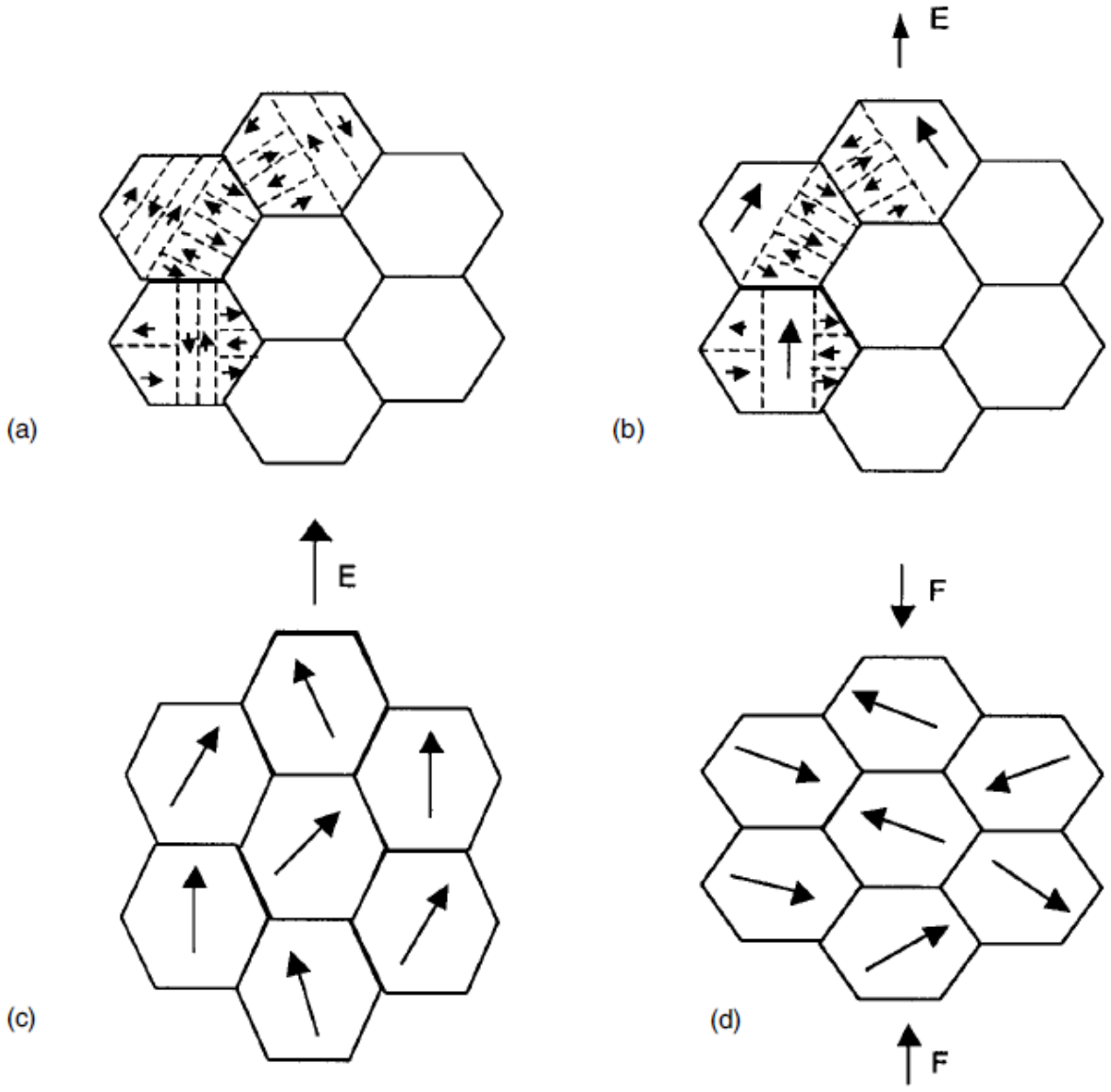

Schematic illustrating the changes accompanying the application of electrical and mechanical stresses to a polycrystalline ferroelectric ceramic:

(a) stress-free – each grain is non-polar because of the cancellation of both 180° and 90° domains;
(b) with applied electric field – 180° domains switch producing net overall polarity but no dimensional change;
(c) with increase in electric field, 90° domains switch accompanied by small (1%) elongation;
(d) domains disorientated by application of mechanical stress.

Polished and etched unpoled ceramic.

$BaTiO_3$: ferroelectric domains

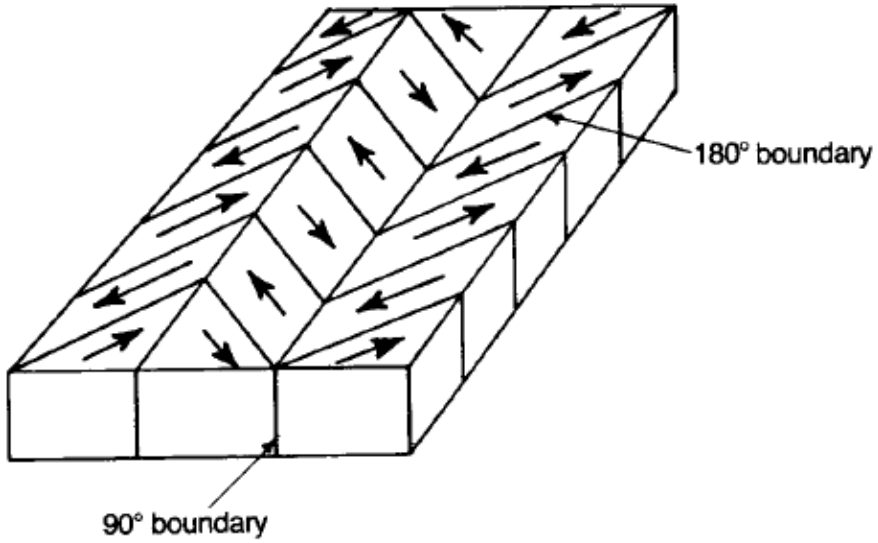

Domain wall (≈10 nm)

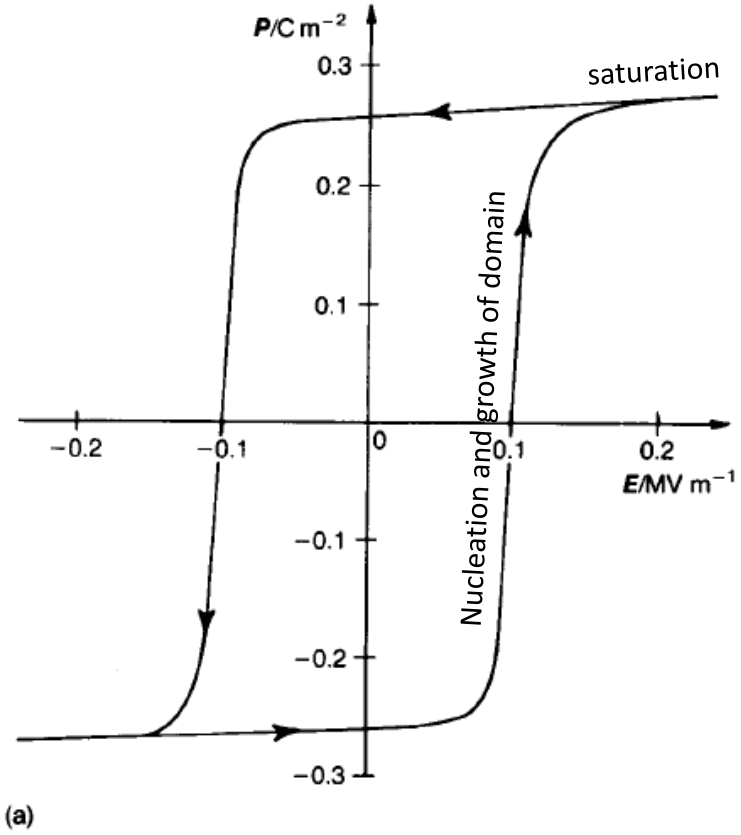

Single domain

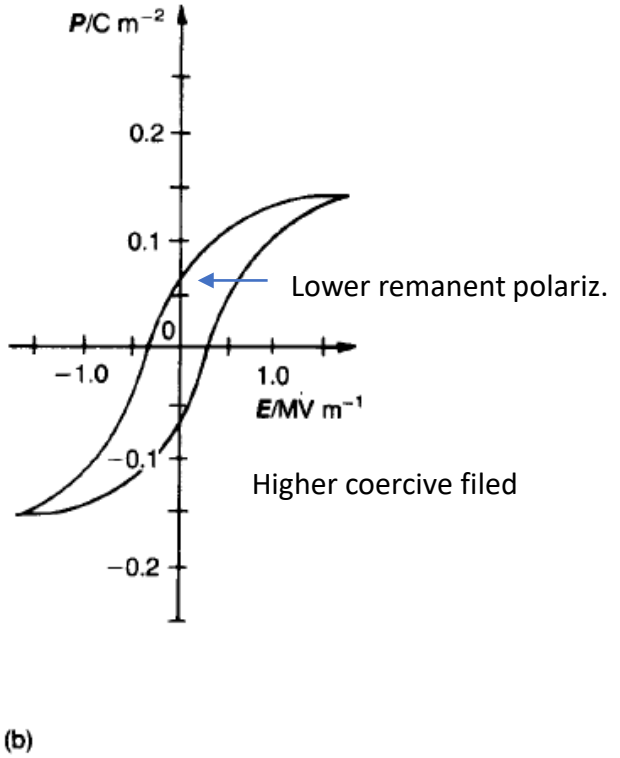

Ceramics

The detailed geometry and dynamics of changes in domain configuration in a single crystal accompanying changes in applied field are complex and there is marked hysteresis between induced polarization and an applied field of sufficient strength. Conditions in a crystallite clamped within a ceramic are even more complex.

Tuning Tc

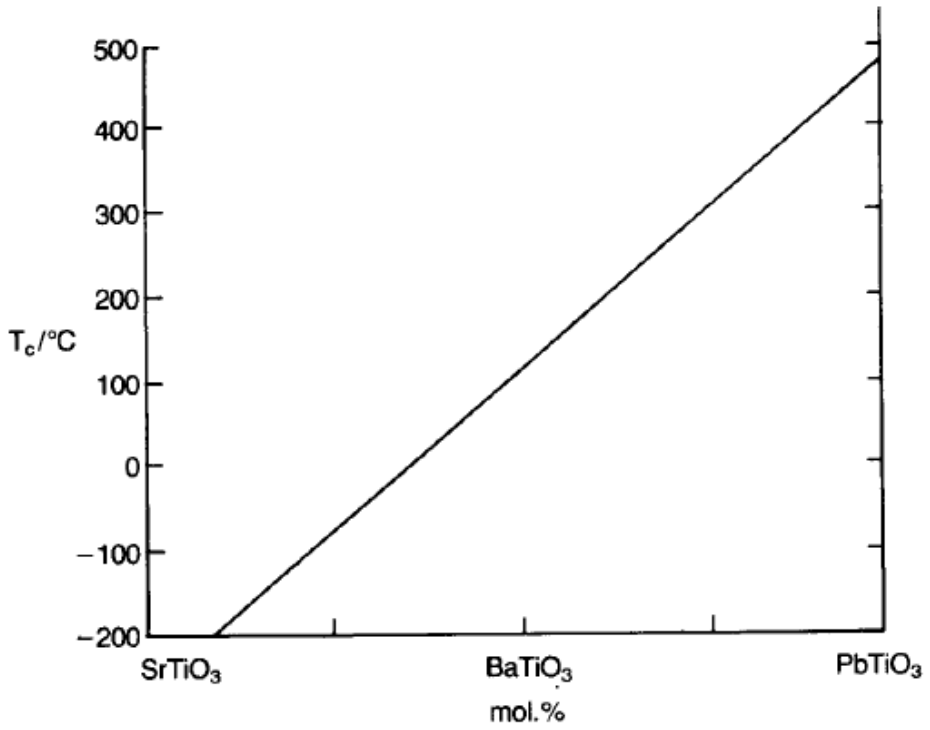

One very significant advantage of ceramic ferroelectrics is the ease with which their properties can be modified by adjusting the composition and the ceramic microstructure. Additions and the substitution of alternative cations can have the following effects:

1. shift the Curie point and other transition temperatures;
2. restrict domain wall motion;
3. introduce second phases or compositional heterogeneity;
4. control crystallite size;
5. control the oxygen content and the valency of the Ti ion.

Grain size effect

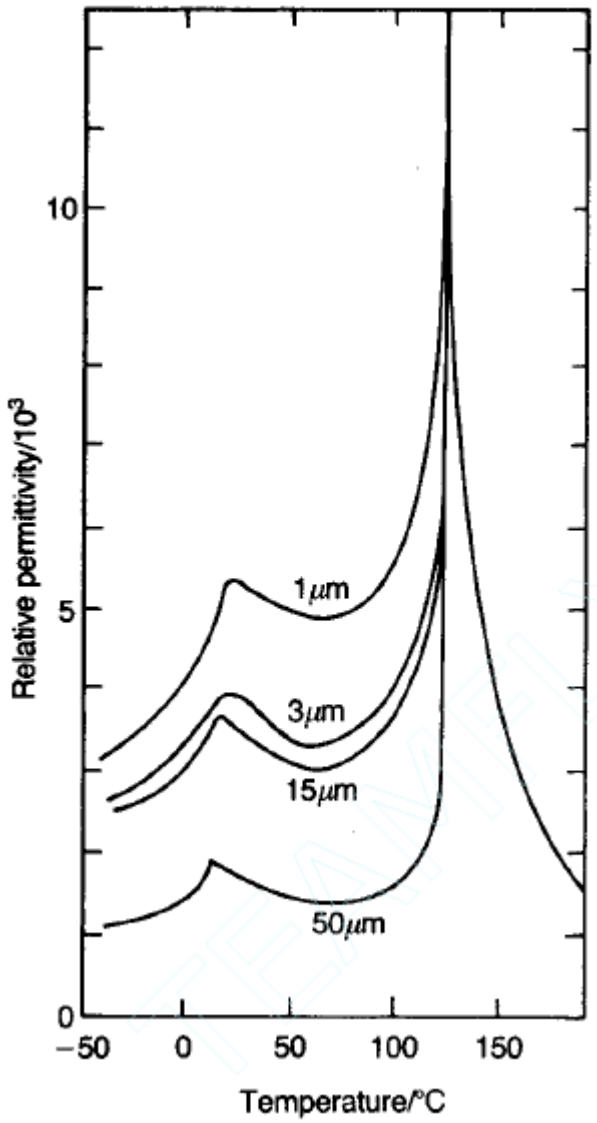

Cations that have a higher valency than those they replace, when present at levels exceeding about 0.5 cation percent, e.g. La^{3+} in place of Ba^{2+} or Nb^{5+} in place of Ti^{4+}, generally inhibit crystal growth. This has the effect of raising the permittivity level below the Curie point as shown in the figure. Crystal size is also controlled by sintering conditions. It has important effects on the electro-optical behavior.

Kröger–Vink defect notation

Table B.1 *The Kröger–Vink notation for defects in crystals*

Defect type	Notation	Defect type	Notation
Metal vacancy at metal (M) site	V_M	Non-metal vacancy at non-metal (Y) site	V_Y
Impurity metal (A) at metal (M) site	A_M	Impurity non-metal (Z) at non-metal (Y) site	Z_Y
Interstitial metal (M)	M_i	Interstitial non-metal (Y)	Y_i
Neutral metal (M) vacancy	V_M^x	Neutral non-metal (Y) vacancy	V_Y^x
Metal (M) vacancy with negative effective charge	V_M'	Non-metal (Y) vacancy with positive effective charge	$V_Y^\bullet$
Interstitial metal (M) with *n* positive effective charges	$M_i^{n\bullet}$	Interstitial non-metal (Y) with *n* negative effective charges	$Y_i^{n'}$
Free electron	e'	Free hole	$h^\bullet$
Neutral associated defects (vacancy pair)	$(V_M V_Y)$	Associated defects with positive effective charge	$(V_M V_Y)^\bullet$

Examples:

1. in $SrTiO_3$, the symbol V_{Sr} would represent a strontium atom vacancy;
2. a Ba substituent on an Sr site in $SrTiO_3$ is written as Ba_{Sr}
3. O_i would represent an interstitial oxygen atom in $La_2CuO_{4+\delta}$
4. Associated lattice defects are in parentheses
5. The superscript ’ is used for each unit of effective negative charge; the superscript • is used for each unit of effective positive charge: La substituent on an Sr site in $SrTiO_3$ would have an effective charge of +1 and be written $La^\bullet_{Sr}$. The charge balance would be maintained by the creation of a Ti^{3+} cation in place of a Ti^{4+} cation, written Ti'_{Ti}
6. Electrons and holes are denoted by the symbols e' and $h^\bullet$
7. Oi'' would represent an interstitial O^{2-} anion in $La_2CuO_{4+\delta}$
8. A defect that has no effective charge can be given the (optional) superscript *x*

Ion incorporation in BT into A-site

The mechanism of dopant incorporation into BT has been extensively investigated and the behavior of some transition-metal ions as well as that of the larger rare-earth ions has been well elucidated. The ionic radius is the parameter which mainly determines the substitution site. La^{3+} (1.15 Å) and Nd^{3+} (1.08 Å) are exclusively incorporated at the Ba^{2+} (1.35 Å) site, as their size is incompatible with that of Ti^{4+} (0.68 Å). In fact, it has long been known that La^{3+} and Nd^{3+}, when added in small amounts (<0.5at.%), behave as **donors** and lead to room-temperature semiconducting ceramics (electron compensation) with positive temperature coefficient of resistivity (PTCR).

$$M_2O_3 + 2TiO_2 \rightarrow 2M^{\bullet}_{Ba} + 2e' + 2Ti_{Ti} + 6O_O + \frac{1}{2}O_2$$

Compensation defect: e (conductive)

When the dopant concentration increases, the material becomes insulating, and the transition is accompanied by grain growth inhibition. In heavily doped materials, charge compensation takes place by barium (V''_{Ba}) or titanium (V''''_{Ti}) vacancies

$$M_2O_3 + 3TiO_2 \rightarrow 2M^{\bullet}_{Ba} + V''_{Ba} + 3Ti_{Ti} + 9O_O$$

$$2M_2O_3 + 3TiO_2 \rightarrow 4M^{\bullet}_{Ba} + V''''_{Ti} + 3Ti_{Ti} + 12O_O$$

Compensation defect: V (insulator)

Buscaglia et al, J. Am. Ceram. Soc., 85 [6] 1569 –75 (2002)

Ion incorporation in BT into B-site

The transition series ions Cr^{4+}(0.55 Å), Fe^{3+}(0.64 Å), Co^{2+} (0.78 Å), Co^{3+} (0.63 Å), Mn^{2+} (0.83 Å), Mn^{3+} (0.64 Å), Mn^{4+}(0.53 Å), Ni^{2+}(0.78 Å), Nb^{5+} (0.64 Å), and Ta^{5+} (0.64 Å),because of their small size, give exclusive substitution on the Ti (B) site.
In particular, Nb^{5+} is added as a **donor** in small concentrations(<0.3 at.%) to obtain semiconducting ceramics.

$$M_2O_5 + 2BaO \longrightarrow 2M_{Ti}^{\cdot} + 2e' + 2Ba_{Ba} + 6O_o + \frac{1}{2}O_2$$

Compensation defect: e (conductive)

while Ni^{2+}, Co^{2+}, Co^{3+}, Fe^{3+}, and Mn^{2+} act as **acceptors** and give insulating materials at room temperature. The positive excess charge of the acceptor ion at the Ti site is mainly compensated by creation of oxygen vacancies ($V_O^{\cdot\cdot}$)

$$M_2O_3 + 2BaO \rightarrow 2M_{Ti}' + V_O^{\cdot\cdot} + 2Ba_{Ba} + 5O_O$$

Ion incorporation in BT into A&B-sites

For Y^{3+} and lanthanide ions of intermediate size, from Sm^{3+} (1.04 Å) to Er^{3+} (0.96 Å), there are some indications that the substitution site is not exclusive, but is affected by dopant concentration, sintering temperature, sintering atmosphere, and Ba/Ti molar ratio (which play a major role). Self-compensation is possible.

$$M_2O_3 \rightarrow M_{Ba}^{\bullet} + M_{Ti}' + 3O_O$$

These dopants are called “magic dopants”: since they can be incorporated in both sites can adjust small stoichiometry mismatch and increase in general the stability of the material.

Positive temperature coefficient resistors (PTCR)

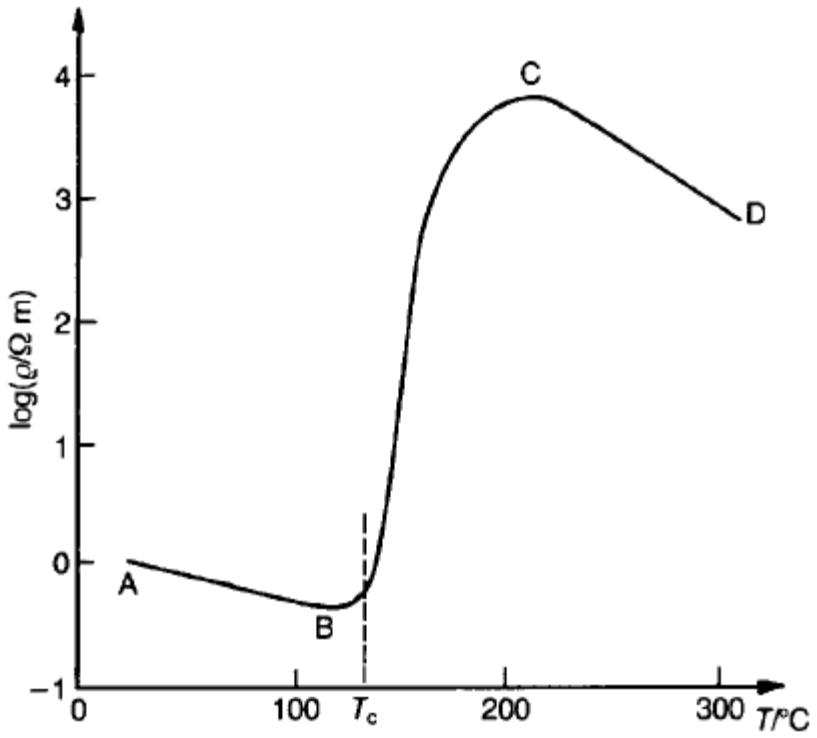

Fig. 4.20 Typical characteristic of PTC thermistor material.

In the figure the material has the negative resistivity temperature characteristic associated with normal semiconductors up to about 100 °C (AB) and above about 200 °C (CD), while between these temperatures (BC) there is an increase of several orders of magnitude in resistivity.

The PTC effect is exhibited by specially doped and processed $BaTiO_3$. Because the effect is not observed in the single-crystal form of the material, its cause must be assumed to lie in processes associated with grain boundaries. Attention here is focused on lanthanum-doped $BaTiO_3$ (BLT), although other donor dopants would be satisfactory, e.g. yttrium (A site) or niobium, tantalum or antimony (B site).

Positive temperature coefficient resistors (PTCR)

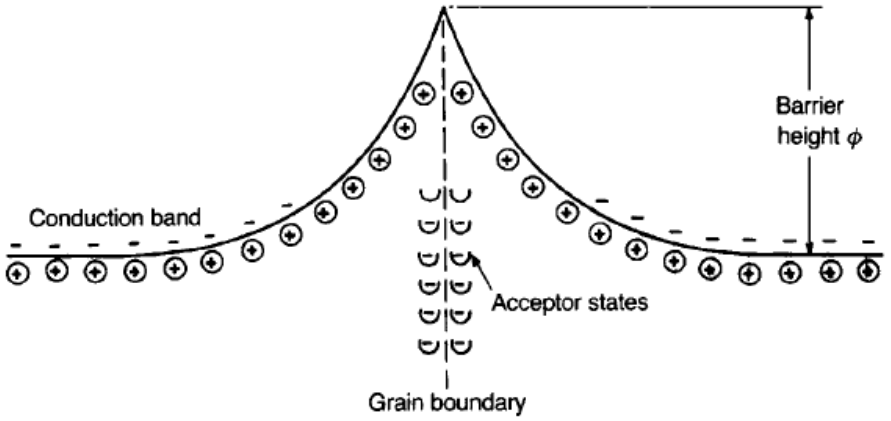

Electron acceptor states in the grain boundary together with nearby ionized donor states give rise to an electrical double layer.
Thus, conduction band electrons moving up to a grain boundary from the interior of a grain are confronted by a potential barrier of height ϕ

The PTC effect is seen to have its origins in the resistance of the grain boundary region which increases exponentially with temperature above the ferroelectric–paraelectric transition temperature. It therefore depends on the number of grain boundaries per unit volume of ceramic, i.e. on the microstructure, and of course on the acceptor and donor state densities.

Current voltage behavior of a PTCR body

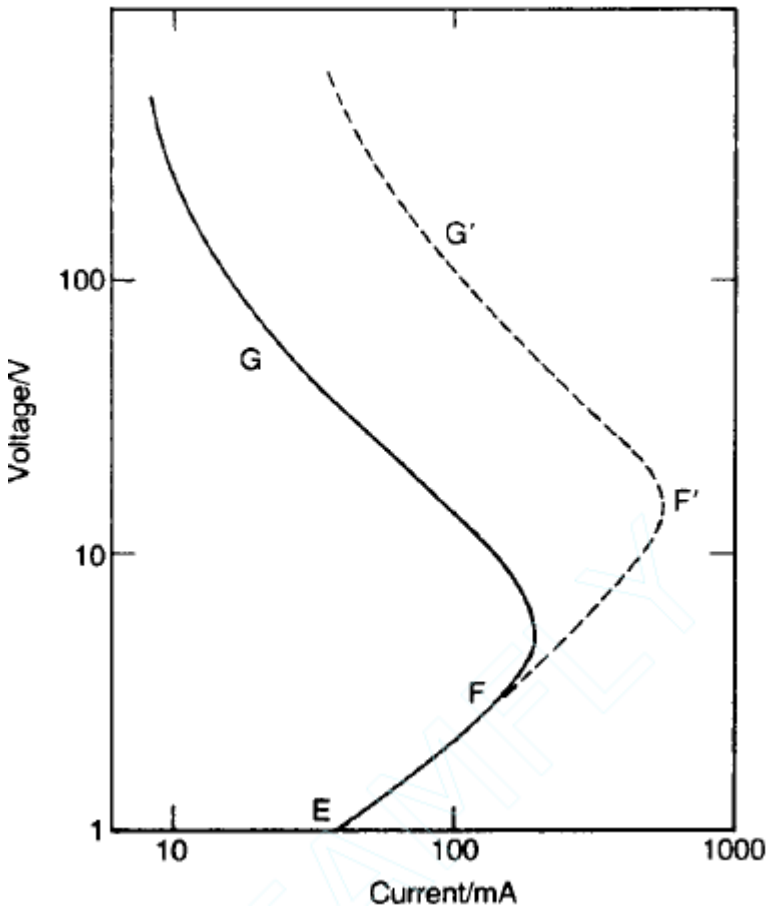

At low voltages (EF) the relation is approximately ohmic (Fig. 4.20, AB); then, as the temperature of the thermistor reaches the regime of steeply rising resistance (Fig. 4.20, BC), its temperature rises only slowly with increasing voltage and the current falls to give a correspondingly slow increase in power dissipation. If the increase in voltage is sufficient to bring the temperature above the region of rising resistance (Fig. 4.20, CD), the temperature coefficient becomes negative and a rapid increase in current and temperature results.

If the rate of heat dissipation from the thermistor is changed, the location of FG will shift. The temperature of the element changes only slightly, but the power changes to a level corresponding to the new rate of heat dissipation. If the voltage is kept constant the current becomes a measure of the rate of heat dissipation, and this relation is used in a number of devices to sense a change in environment. There is a marked change in heat dissipation when a probe at thermal equilibrium in air is plunged into a liquid at the same temperature as the air. Devices for indicating the level of liquids in tanks are based on this change.

Ohmic: R = V/I

PTCR as heating elements or sensor

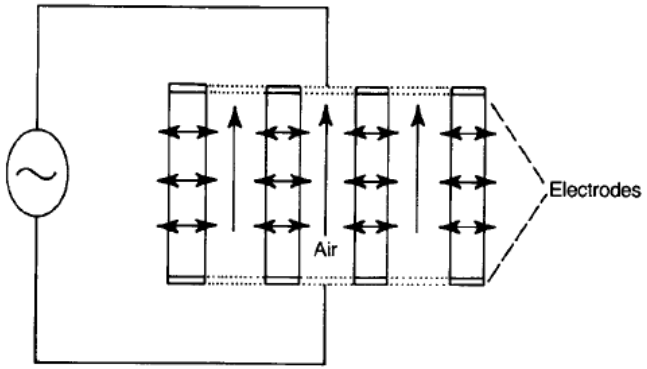

The relative constancy in the temperature of a PTC device, despite changes in both the voltage supply and ambient conditions, when it is maintained on the steeply rising limb of its resistance–temperature characteristic has led to its use as a heating element in miniature ovens for quartz crystals acting as constant frequency sources. It has also been made use of in hair-driers and space-heaters.

Air is blown through the perforations in a block of ceramic that is designed to heat the emergent air to a suitable temperature. Even when the fan is switched off the heater temperature only rises by about 20 °C so that no damage results.

PTC elements make useful temperature indicators because the sharp rise in resistivity above the Curie point is very easily detected or used to operate a control mechanism.

PTCR kit

PTCR for automotive

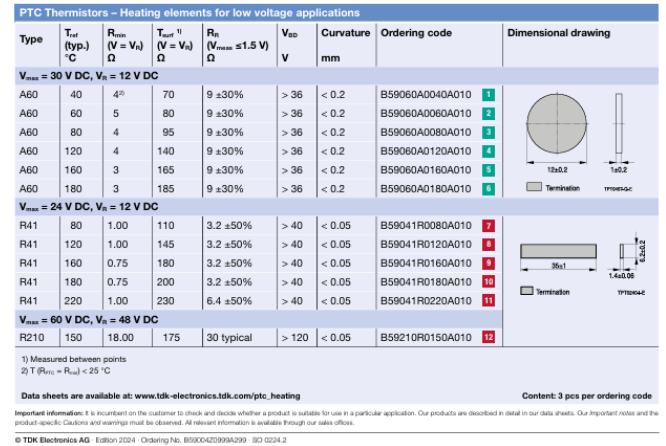

PTC Thermistors – Heating elements for low voltage applications

Type	T_{ref} (typ.) °C	R_{min} ($V = V_R$) Ω	T_{ref} [1] ($V = V_R$) Ω	R_R ($V_{max} \leq 1.5$ V) Ω	V_{RD} V	Curvature mm	Ordering code	
V_{max} = 30 V DC, V_R = 12 V DC								
A60	40	4[2]	70	9 ±30%	> 36	< 0.2	B59060A0040A010	1
A60	60	5	80	9 ±30%	> 36	< 0.2	B59060A0060A010	2
A60	80	4	95	9 ±30%	> 36	< 0.2	B59060A0080A010	3
A60	120	4	140	9 ±30%	> 36	< 0.2	B59060A0120A010	4
A60	160	3	165	9 ±30%	> 36	< 0.2	B59060A0160A010	5
A60	180	3	185	9 ±30%	> 36	< 0.2	B59060A0180A010	6
V_{max} = 24 V DC, V_R = 12 V DC								
R41	80	1.00	110	3.2 ±50%	> 40	< 0.05	B59041R0080A010	7
R41	120	1.00	145	3.2 ±50%	> 40	< 0.05	B59041R0120A010	8
R41	160	0.75	180	3.2 ±50%	> 40	< 0.05	B59041R0160A010	9
R41	180	0.75	200	3.2 ±50%	> 40	< 0.05	B59041R0180A010	10
R41	220	1.00	230	6.4 ±50%	> 40	< 0.05	B59041R0220A010	11
V_{max} = 60 V DC, V_R = 48 V DC								
R210	150	18.00	175	30 typical	> 120	< 0.05	B59210R0150A010	12

1) Measured between points
2) T (R_{min} = R_{ref}) < 25 °C

Data sheets are available at: www.tdk-electronics.tdk.com/ptc_heating

Content: 3 pcs per ordering code

Co-firing example: 5 layers active component

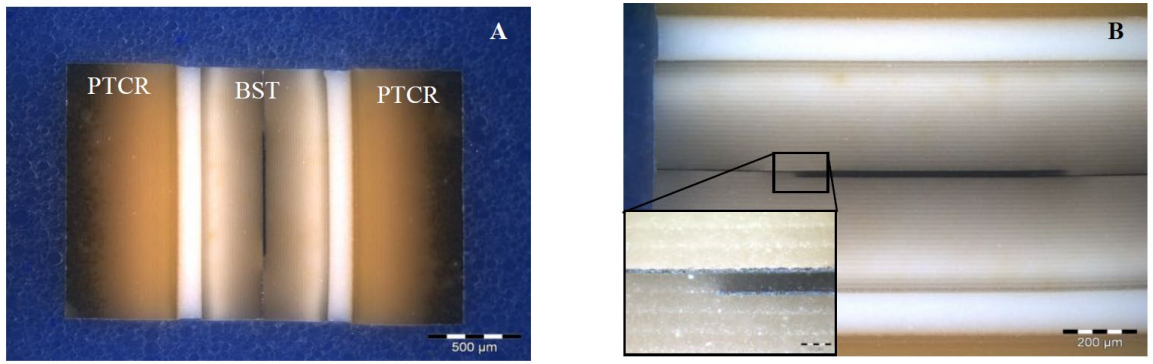

Figure 3 – Device cross sections: (A) overall view, (B) magnification of the inner electrodes' area.

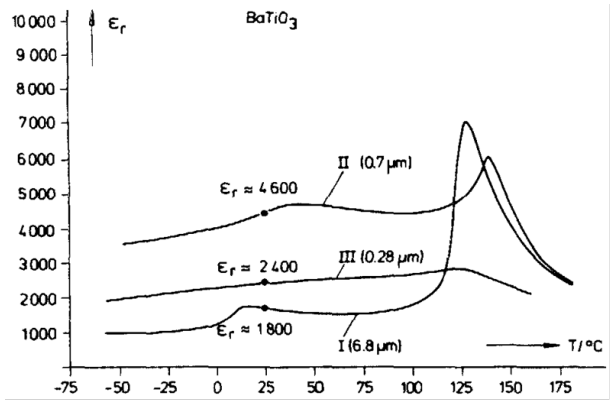

Dielectric constant vs. temperature of $BaTiO_3$ ceramic showing various grain sizes

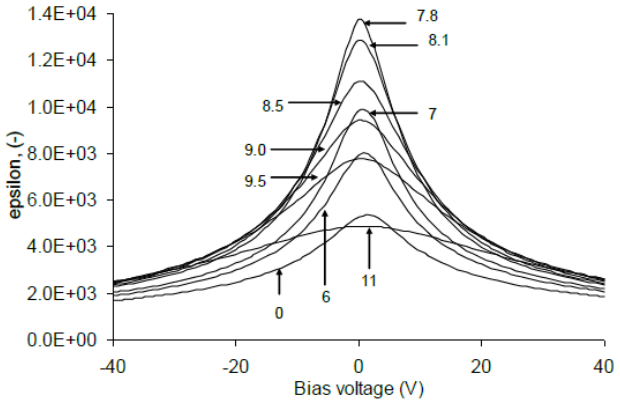

Figure 5 – Dielectric permittivity against $Bias_V$ at different PTC_V (Frequency 200 KHz)

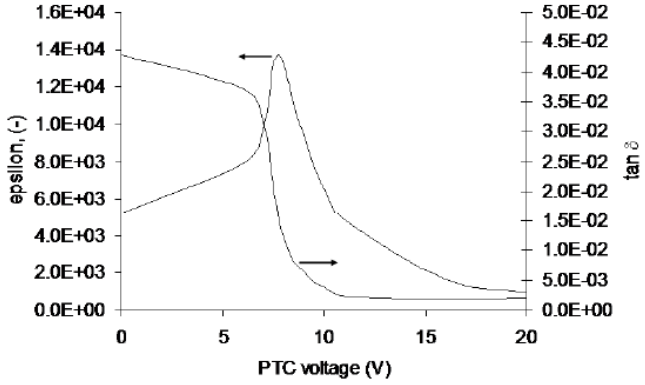

Figure 4 – Dielectric permittivity and dielectric loss against the PTC_V (Frequency 200 KHz)

High Performance Varactor
Andrea Testino
TDK-EPC, Corporate Material R&D – Innovative Themes, Deutschlandsberg, Austria
andrea.testino@epcos.com

(12) United States Patent
Testino
(10) Patent No.: US 8,988,849 B2
(45) Date of Patent: Mar. 24, 2015
(54) VARACTOR AND METHOD FOR PRODUCING A VARACTOR
USPC 361/277, 278, 28

Thermomechanical analysis (TMA) / Dilatometry

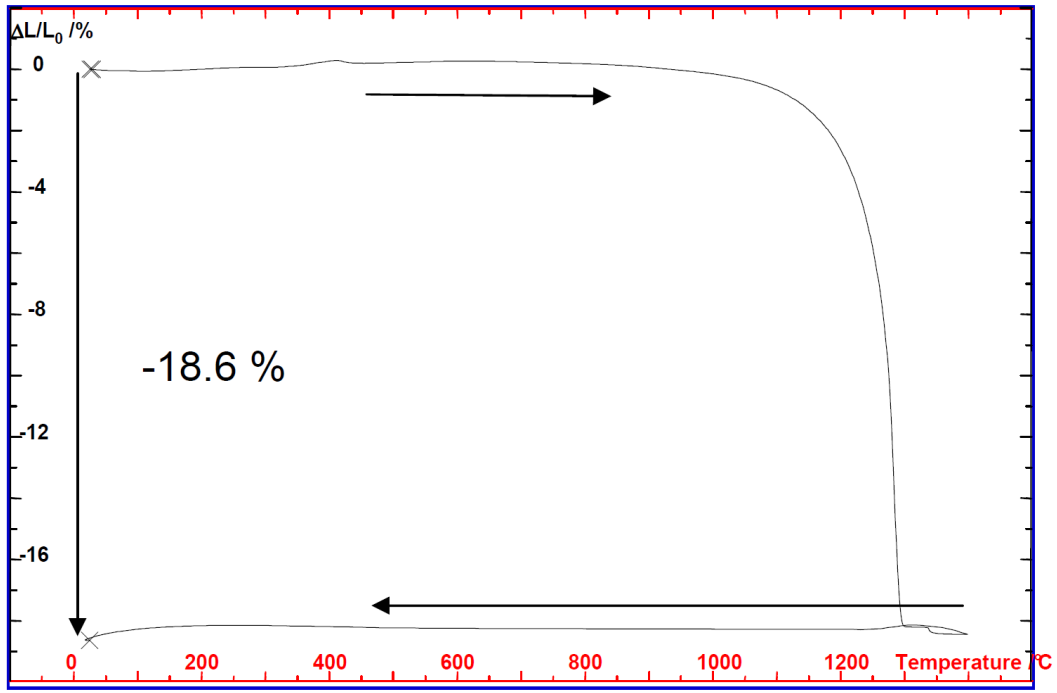

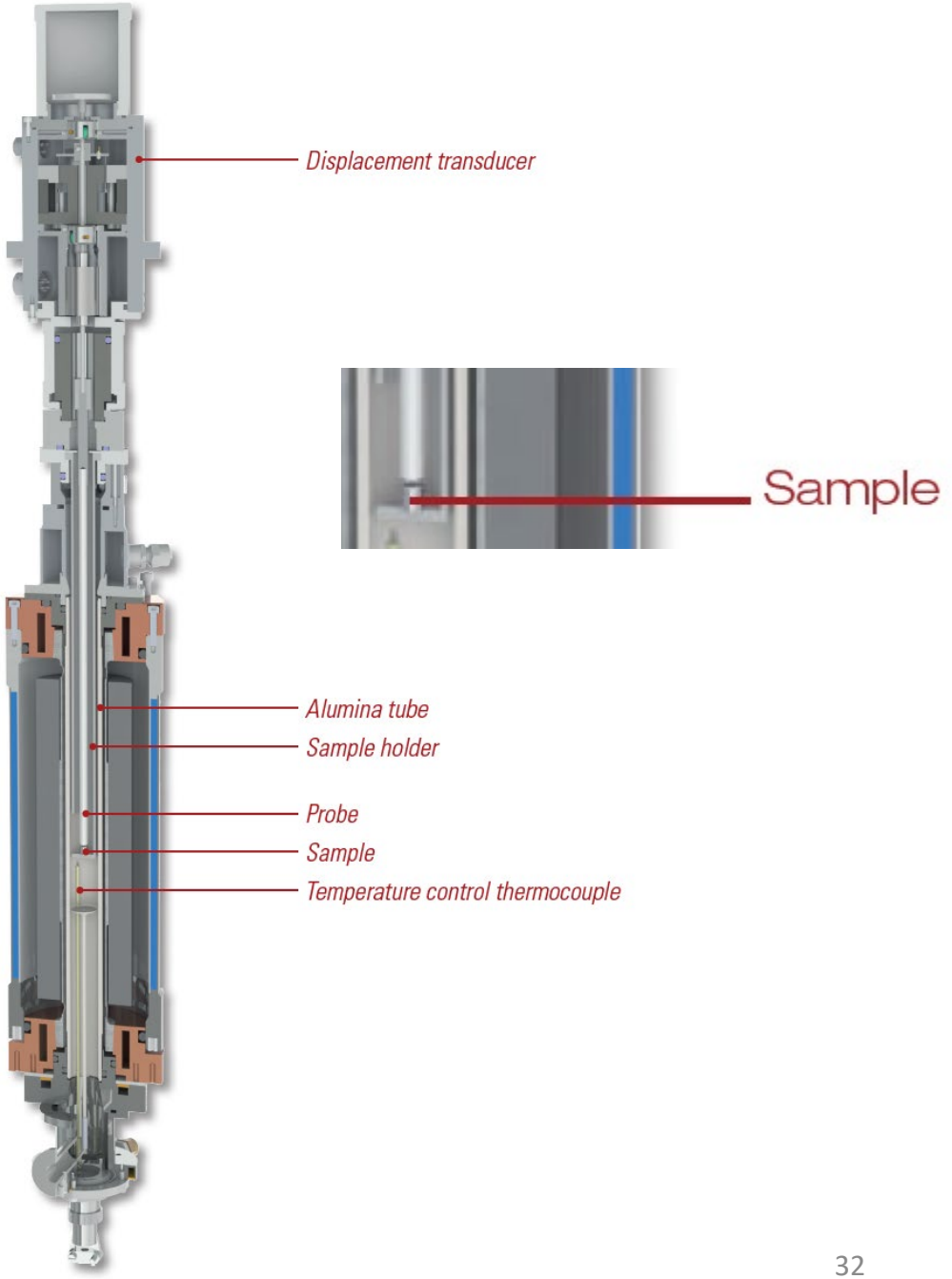

Controlled sintering rate

Properties of a material are improved by maintaining a constant and slow rate of shrinkage during the sintering process. Key parameters are maximum heating rate and sintering rate. The heating rate can be automatically lowered to follow predefined sintering rate and reincreased at the end of the process. This mode is used to generate an optimized temperature profile and to simulate the sintering process.

Co-firing: key (starting) points

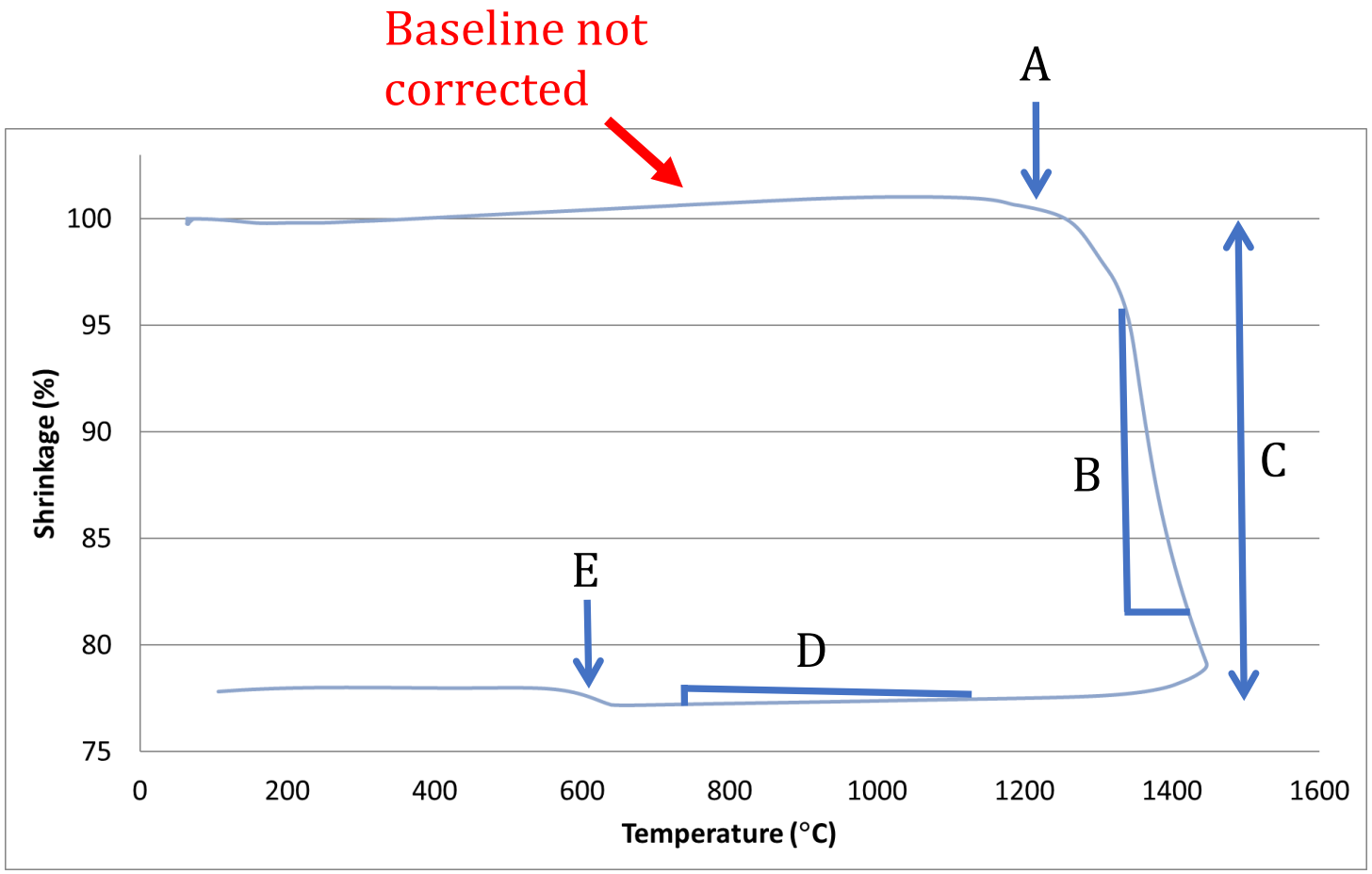

A: sintering onset
B: shrinkage speed
C: overall shrinkage
D: thermal expansion on cooling
E: eventually, phase transitions

A…E: parameters have to match between materials to be co-fired.
No match → cracks, delamination, failure

Hybrid Organic-Inorganic Perovskites

Table 1.6 *Organic–inorganic hybrid and related perovskites*

Phase	Space group	a (nm)	b (nm)	c (nm)	Angles (°)	Cubic transition Temp (K)
$CsSnI_3$	O, *Pnma* (62)	0.86885	1.23775	0.86384		300
$CsSnI_3$	T, *P4/mbm* (127)	0.87182		0.61908		350
$CsSnI_3$	C, *Pm$\bar{3}$m* (221)	0.62057				478
$MAGeCl_3$	M, *P2$_1$/n* (14)	1.09973	0.72043	0.82911	α, 90.47	2
$MAGeCl_3$	O, *Pmna* (62)	1.11567	0.73601	0.82936		250
$MAGeCl_3$	Tr, *R3m* (160)	0.56784			α, 90.95	370
$MAGeCl_3$	C, *Pm$\bar{3}$m* (221)	0.56917				475
$CD_3ND_3GeCl_3$	M, *P2$_1$/n* (14)	1.09973	0.72043	0.82911	β, 90.47	2
$CD_3ND_3GeCl_3$	O, *Pnma* (62)	1.11567	0.73601	0.82936		250
$CD_3ND_3GeCl_3$	Tr, *R3m* (160)	0.56584			α, 90.95	370
$CD_3ND_3GeCl_3$	C, *Pm$\bar{3}$m* (221)	0.56917				475
$MASnCl_3$	Tri, *P1* (1)	0.5726	0.8227	0.7910	α, 90.40 β, 93.08 γ, 90.15	297
$MASnCl_3$	M, Pc (7)	0.5718	0.8326	0.7938	β, 93.03	318
$MASnCl_3$	Tr, *R3m* (160)	0.5734			α, 91.90	350
$MASnCl_3$	C, *Pm$\bar{3}$m* (221)	0.5760				478
$MASnBr_3$	O, *Pmc2$_1$* (26)	0.58941	0.83862	0.82406		215
$MASnI_3$	T, *P4mm* (99)	0.62302		0.6231		293
$MASnI_3$	T, *I4cm* (108)	0.87577		1.2429		200
$MAPbI_3$	T, *P4mm* (99)	0.63115		0.63161		400
$MAPbI_3$	T, *I4cm* (108)	0.8849		1.2642		293
$MAPbI_3$	O, *Pmna* (62)	0.88362	1.25804	0.85551		100
$FASnI_3$	O, *Amm2* (38)	0.63286	0.89554	0.89463		340
$FASnI_3$	O, *Imm2* (44)	1.25121	1.25171	1.25099		180
$CH_3ND_3PbCl_3$	O, *Pnma* (62)	1.11747	1.13552	1.12820		80
$CH_3ND_3PbCl_3$	C, *Pm$\bar{3}$m* (221)	0.5669				280
$CH_3ND_3PbBr_3$	O, *Pnma* (62)	0.79434	1.18499	0.85918		11
$MAPbI_3$	O, *Pnma* (62)	0.88362	1.25804	0.85551		100
$MAPbI_3$	T, *I4/mcm* (140)	0.8851		1.2444		298
$MAPbI_3$	C, *Pm$\bar{3}$m* (221)	0.6274				333
$FAPbI_3$	Tr, *P3m1* (156)	0.89817		1.1006	γ, 120	293

The A-sites in the perovskite structure are large enough to accommodate a number of complex ions including ammonium $(NH_4)^+$; methyl ammonium $(CH_3NH_3)^+$ frequently written as MA; tetramethylammonium, $[(CH_3)_4N]^+$, frequently written as TMA and formamidinium $(NH2{=}CHNH_2)^+$, written as FA.
The most important of these are the compounds formed with the Group 14 elements Ge, Sn and Pb, together with a halogen Cl, Br and I.

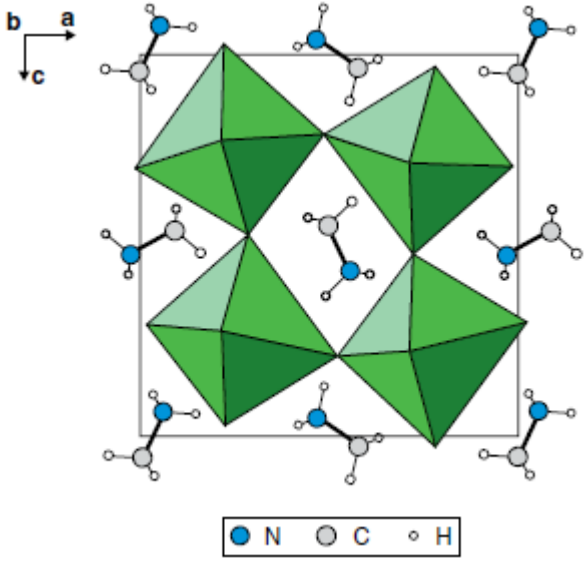

The structure of ($MAPbCl_3$). One layer of the structure is shown. In preceding and succeeding layers, the organic molecules are rotated by 180° compared to that drawn.

This class of materials is well-known for the assembly of perovskite solar cell (https://en.wikipedia.org/wiki/Perovskite_solar_cell)

Structure-Field Maps (related to the tolerance factor)

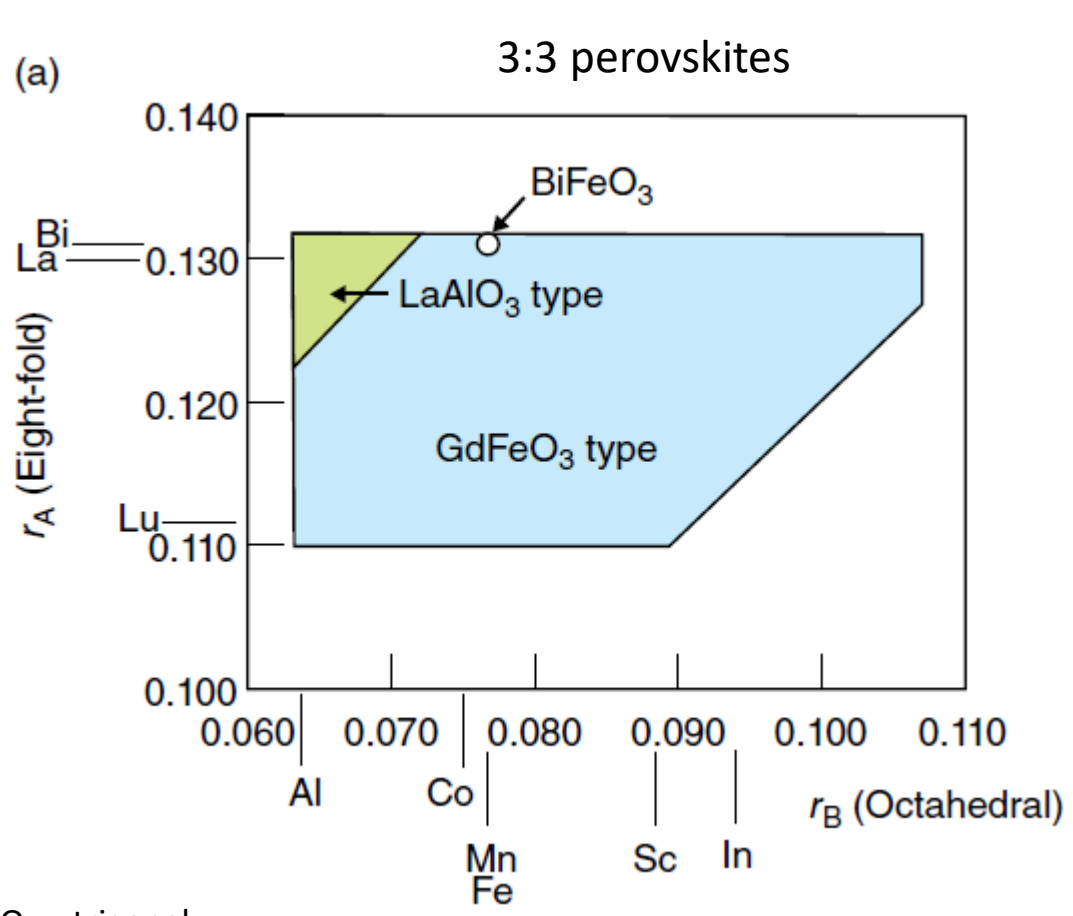

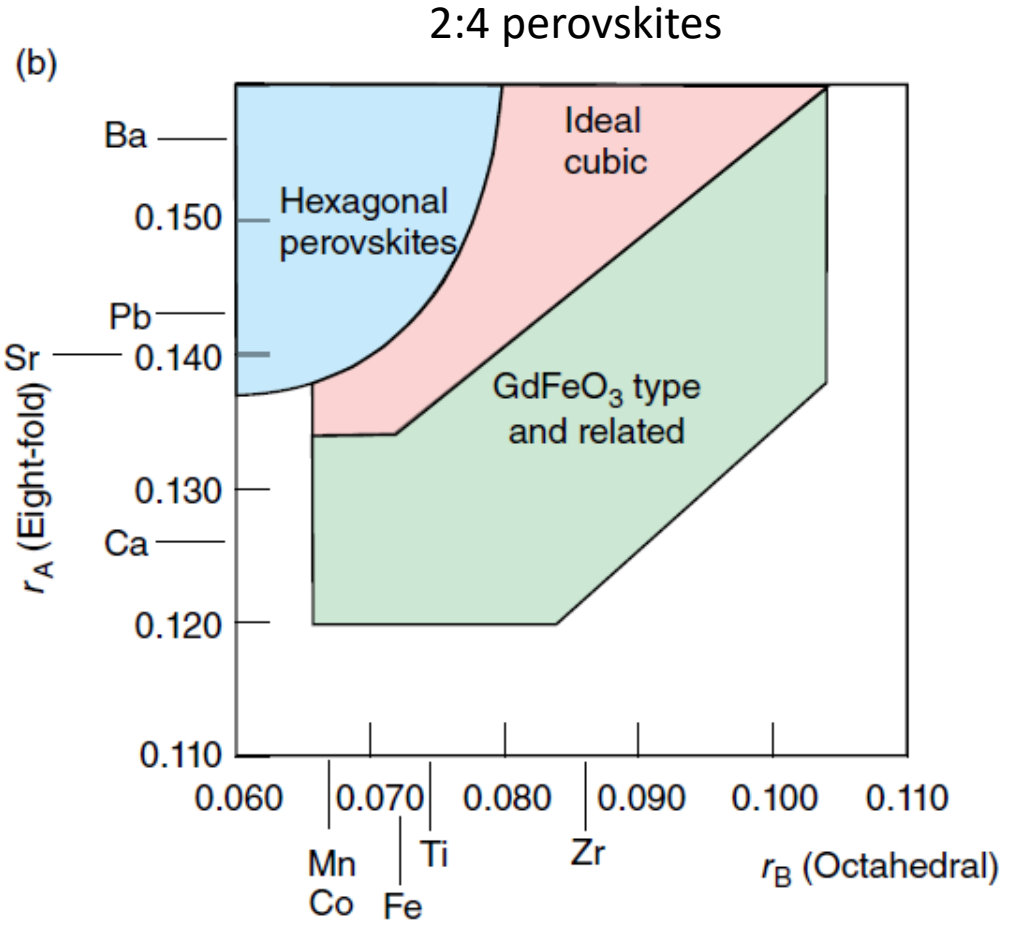

$LaAlO_3$: trigonal
$GdFeO_3$: orthorhombic
$BiFeO_3$: rhombohedral (anomaly)

The radii appropriate to the y-axis, associated with the A cations, should refer to 12-fold coordination. As such radii are not widely available, the figures here use eightfold radii on this axis.

Perovskite vs. non-perovskites

Recent efforts have used plots of the tolerance factor against the ratio of the radii of the B-site cation to the X-site anion as an octahedral factor (μ) :

$$\mu = \frac{r_B}{r_X}$$ radii of the B-site cation to the X-site anion

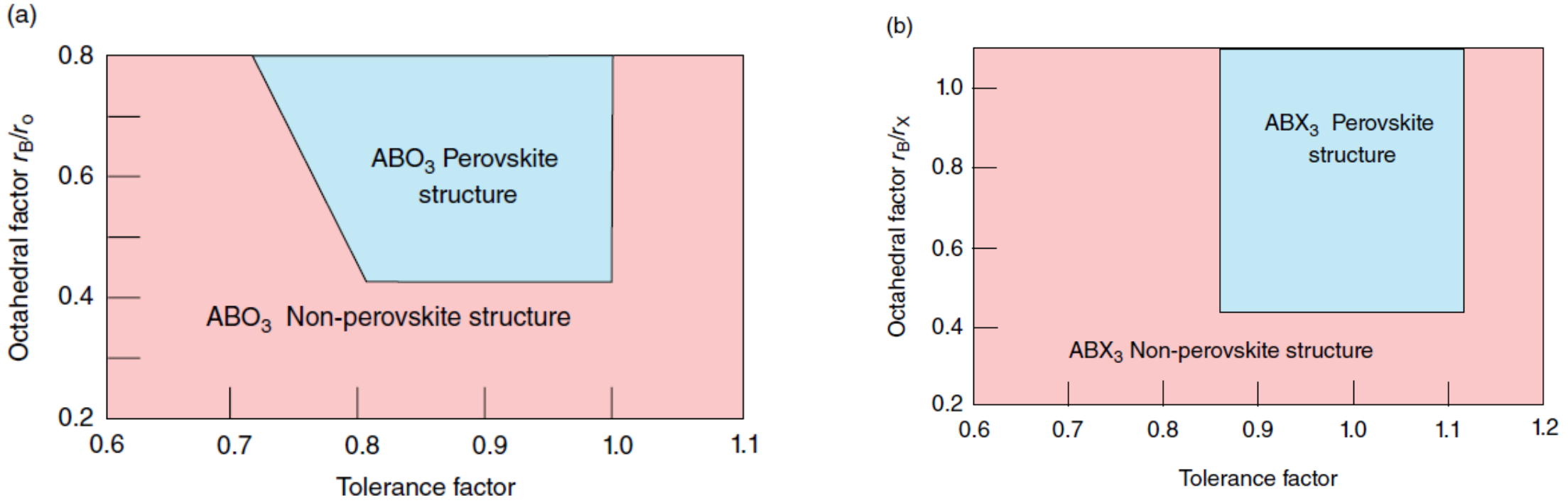

Although structure-field maps do not predict the existence of the perovskite form with complete certainty, indicating that the factors that endow stability to this structure lie outside of simple radius correlations, the ease of the method makes it a simple and useful guide when unknown systems are being explored.

Perovskite: BT synthesis as example

1. “Mixed oxide” or solid-state route

$$BaCO_3 + TiO_2 \longrightarrow BaTiO_3 + CO_2$$

T ≈ 1100 °C

In case of NPs, T can be decreased to 700 °C [1] obtaining ceramic BT with size ≈ 70 nm (!)

Advantages: easy, large scale, very well established. But: relatively high T, milling needed to obtain an average size ≈ 1 μm

2. Oxalate route

$$BaCl_2 + TiOCl_2 + 2C_2O_4H_2 + 4H_2O \longrightarrow BaTiO(C_2O_4)_2 \cdot 4H_2O \downarrow + 4HCl$$ Overall reaction

$$BaTiO(C_2O_4)_2 \cdot 4H_2O \longrightarrow BaTiO(C_2O_4)_2 + 4H_2O$$ De-hydration 100-140 °C

$$2BaTiO(C_2O_4)_2 \longrightarrow BaTi_2O_5 + BaCO_3 + 4CO + 3CO_2$$ Decomposition 300-350 °C

$$BaTi_2O_5 + BaCO_3 \rightarrow 2\,BaTiO_3 + CO_2$$ BT formation 600-800 °C

Advantages: lower T, smaller particle. But: care need to be taken during thermal treatment

[1] J. Am. Ceram. Soc., 91 [9] 2862–2869 (2008)

Perovskite: BT synthesis as example

3. Alkoxide route Different alkoxide can be used, typically isopropoxide, butoxide

$Ti[OCH(CH_3)_2]_4$ $Ti(OCH_2CH_2CH_2CH_3)_4$

$$Ba(OH)_2 + Ti(OR)_4 + H_2O \rightarrow BaTiO_3 + 4ROH$$

In general $Ti(OR)_4$

The reaction can be strongly exothermic, additional mineralized (NaOH) might be used. Small particles can be produced, but relatively high-cost precursors. Butoxide route very interesting and largely tested. Very often a post-treatment is needed, such as a calcination step at relatively low temperature to convert the material into fully crystalline BT. This treatment induce a certain degree of aggregation. Gently milling would be required.

4. Hydrothermal route

It is a relatively low-temperature method (100-250 °C) but autoclaves are needed (close pressured reactor). The pressure is typically the autogenous pressure generated in a closed reactor. Essentially, a Ba salt (such as chloride), a Ti precursor (such as $TiOCl_2$) and a mineralizer (such as NaOH) are mixed in a reactor and let react under hydrothermal conditions for few hours. The quality of the material obtained strongly depends on the experimental conditions, but it is typically well crystallized, and no thermal treatment is required.

$$BaCl_2 + TiOCl_2 + 4NaOH \rightarrow BaTiO_3 + 4NaCl + H_2O$$ 100 > T (°C) > 250 1 < P (bar) < 30 pH>12

An excess of mineralizer is needed to set the alkaline pH, which partially remain in the product (e.g., Na contamination)

High entropy perovskites, HEP (high entropy alloy, HEA)

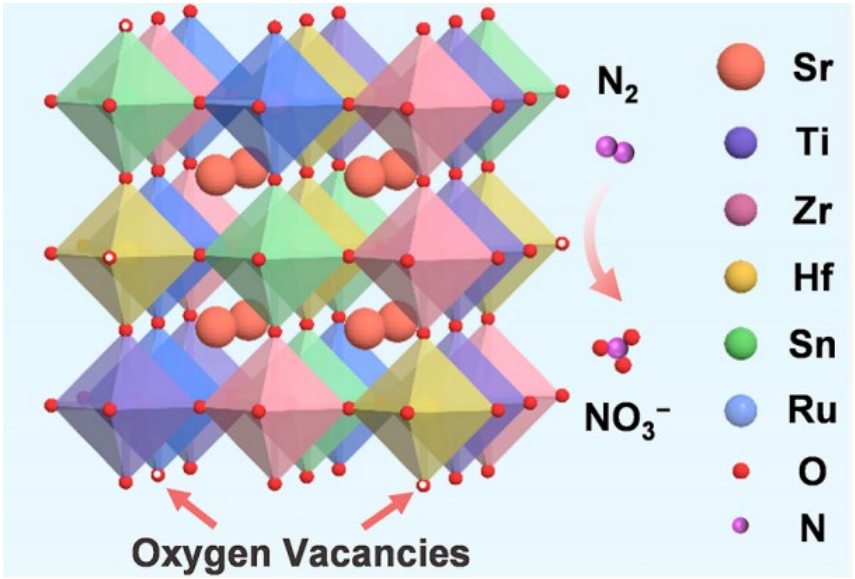

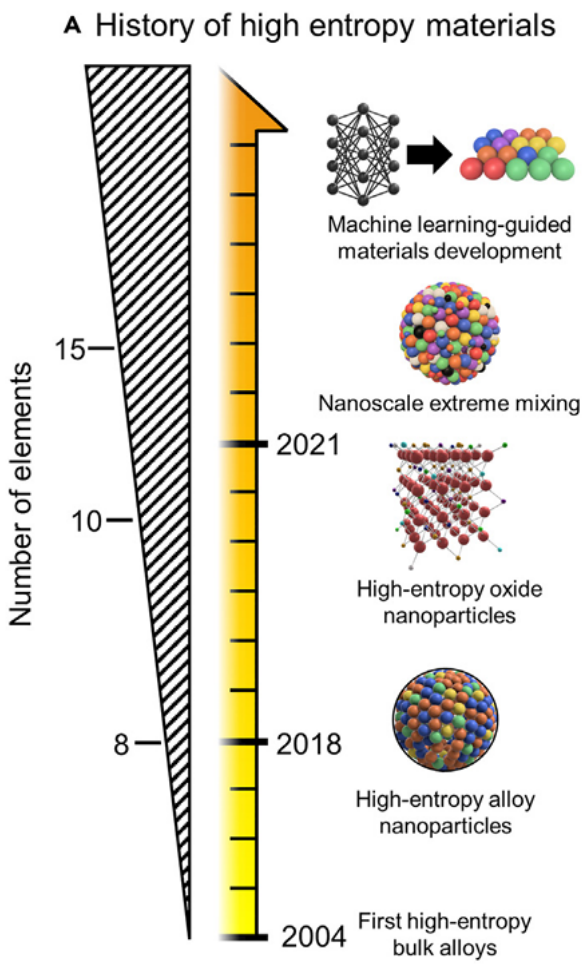

Consider for instance the example

$Sr(Fe_{0.2}Ti_{0.2}Mo_{0.2}Nb_{0.2}Cr_{0.2})O_3$

5 cations on B-site, equal amount

$$t = \frac{r_A + r_O}{\sqrt{2}(r_B + r_O)} = \frac{r_{Sr} + r_O}{\sqrt{2}\left(\frac{r_{Fe} + r_{Ti} + r_{Mo} + r_{Nb} + r_{Cr}}{5} + r_O\right)}$$

$$= 0.906$$

Adapted t factor

A cubic phase is likely to be stable when $0.9 \leq t \leq 1$, while an orthorhombic or rhombohedral phase may form when $t<0.9$, and a tetrahedral or hexagonal phase may form when $t>1$. From the calculated tolerance factor, it is apparent that the stable cubic HEP crystal structure could be formed

ACS Nano 2024, 18, 17642−17650

Joule 7, 843–854, May 17, 2023

ACS Sustainable Chem. Eng. 2020, 8, 17022−17032

High entropy perovskites

Configuration entropy: $$\Delta S_{conf} = -R\left[\left(\sum_{i=1}^{N} x_i ln(x_i)\right)_{cation-site} + \left(\sum_{j=1}^{M} x_j ln(x_j)\right)_{anion-site}\right]$$

Reduced to: $$\Delta S_{conf} = -R\left[\left(\sum_{i=1}^{N} x_i ln(x_i)\right)_{B-site}\right]$$ in A (x_i) O_3

Being $G = H + TS$ an increase of entropy due to the configurational contribution, leads to a thermodynamic stabilization. HEPs can therefore maintain negative values of G at high sintering temperatures, preventing phase transitions during cooling and forming energetically stable single-phase structures. These stable structures exhibit exceptional chemical and structural stability, making them highly suitable for energy applications.